

Frank Schultz · Bernd Lehmann · Sohrab Tawackoli  
Reinhard Rössling · Boris Belyatsky · Peter Dulski

## Carbonatite diversity in the Central Andes: the Ayopaya alkaline province, Bolivia

Received: 12 December 2002 / Accepted: 16 August 2004 / Published online: 5 November 2004  
© Springer-Verlag 2004

**Abstract** The Ayopaya province in the eastern Andes of Bolivia, 100 km NW of Cochabamba, hosts a Cretaceous alkaline rock series within a Palaeozoic sedimentary sequence. The alkaline rock association comprises nepheline-syenitic/foyaitic to ijolitic intrusions, carbonatite, kimberlite, melilititic, nephelinitic to basanitic dykes and diatremes, and a variety of alkaline dykes. The carbonatites display a wide petrographic and geochemical spectrum. The *Cerro Sapo* area hosts a small calciocarbonatite intrusion and a multitude of ferrocarbonatitic dykes and lenses in association with a nepheline-syenitic stock. The stock is crosscut by a spectacular REE-Sr-Th-rich sodalite-ankerite-baryte dyke system. The nearby *Chiaracke* complex represents a magnesiocarbonatite intrusion with no evidence for a relationship to igneous silicate rocks. The magnesiocarbonatite ( $\Sigma$  REE up to 1.3 wt%) shows strong HREE depletion, i.e. unusually high La/Yb ratios (520–1,500). Calciocarbonatites ( $\Sigma$  REE up to 0.5 wt%) have a flatter REE distribution pattern (La/Yb 95–160) and higher Nb and Zr contents. The sodalite-ankerite-baryte dyke system shows geochemical enrichment features, particularly in Na, Ba, Cl, Sr, REE, which are similar to the unusual

natrocarbonatitic lavas of the recent volcano of Oldoinyo Lengai, Tanzania. The Cerro Sapo complex may be regarded as an intrusive equivalent of natrocarbonatitic volcanism, and provides an example for carbonatite genesis by late-stage crystal fractionation and liquid immiscibility. The magnesiocarbonatite intrusion of Chiaracke, on the other hand, appears to result from a primary carbonatitic mantle melt. Deep seated mantle magmatism/metasomatism is also expressed by the occurrence of a kimberlite dyke. Neodymium and strontium isotope data ( $\epsilon_{Nd}$  1.4–5.4,  $^{87}Sr/^{86}Sr < Bulk$  Earth) indicate a depleted mantle source for the alkaline magmatism. The magmatism of the Ayopaya region is attributed to failed rifting of western South America during the Mesozoic and represents the only occurrence of carbonatite and kimberlite rocks in the Andes.

Editorial Responsibility: J. Hoefs

F. Schultz · B. Lehmann (✉)  
Institute of Mineralogy and Mineral Resources,  
Technical University of Clausthal, Adolph-Roemer-Strasse 2a,  
38678 Clausthal-Zellerfeld, Germany  
E-mail: lehmann@min.tu-clusthal.de  
Tel.: +49-5323-722776  
Fax: +49-5323-722511

S. Tawackoli · R. Rössling  
National Survey for Mining and Geology (SERGEOMIN),  
Casilla, 2729 La Paz, Bolivia

B. Belyatsky  
Institute of Precambrian Geology and Geochronology,  
Russian Academy of Sciences, Makarova 2,  
199034 St Petersburg, Russia

P. Dulski  
GeoForschungsZentrum Postdam, Telegrafenberg,  
14473 Potsdam, Germany

### Introduction

The formation of carbonatite melts is much debated. There is experimental evidence for (1) direct generation of carbonatitic melts by very low degree of partial melting in the mantle, as well as for low-pressure magmatic differentiation of carbonated silicate melts, i.e. (2) liquid immiscibility and (3) crystal fractionation (see, among many others, discussion in Harmer and Gittins 1997; Bell et al. 1998; Bell and Tilton 2001). All three petrogenetic processes are supported by petrological field studies on different carbonatite occurrences (e.g. Bailey 1993; Bell and Keller 1995; Cooper and Reid 1998; Harmer and Gittins 1998; Veksler et al. 1998a). The recent discovery of magnesio- and calciocarbonatites within a few kilometer distance in the Bolivian Andes, together with a wide alkaline rock spectrum, underlines the diversity of the carbonatite family and the coexistence of primary magnesiocarbonatite mantle melts, and of calciocarbonatite exsolved from carbonated nepheline-syenitic melts. Extreme crystal fractionation is documented by

a late sodalite-ankerite-baryte dyke system, which has no known equivalent elsewhere, but shares some petrochemical features of the unique Oldoinyo Lengai natro-carbonatite.

The present study was initiated by the discovery of alluvial diamonds in the Ayopaya region (Lehmann and Schultz 1999). Field work during the last years identified a carbonated kimberlite dyke (see below), but microdiamond testing of a 30-kg-bulk sample of the dyke proved negative and a direct link to diamonds could not be proven so far. In the following sections we will give an overview of the petrology and the geochemistry of the most important magmatic rock types of the Ayopaya alkaline province, with focus on potential diamond-bearing rocks and carbonatite petrogenesis, especially on the Chiaracke carbonatite intrusion and the multiple Cerro Sapo alkaline complex. We will place the Ayopaya alkaline province in a regional tectonic context and will discuss a petrogenetic model for the rock spectrum studied.

## Geological setting

The Ayopaya alkaline province is situated in the eastern Andes of Bolivia, near Independencia, about 150 km SE of La Paz and 100 km NW of Cochabamba. It forms a 50×15 km, NW–SE trending belt between the Santa Rosa and Ayopaya rivers (Fig. 1). The steep landscape is characterised by altitudes from 1,500 to 4,400 m a.s.l. and dense subtropical vegetation reaching up to 3,500 m. Alkaline rocks in the Ayopaya region were first reported by Ahlfeld and Wegener (1931) and Ahlfeld and Mosebach (1935). Ahlfeld rediscovered the spectacular sodalite occurrence of the Cerro Sapo, which had been mined from pre-Incaic to Incaic times. Sodalite gemstones from the Ayopaya region have been found at Tiahuanaco and other historical sites in South America (Ahlfeld and Wegener 1931; Brendler 1932).

The Ayopaya alkaline province is part of a Mesozoic intracontinental rift zone (Fig. 1) stretching from Peru to SE Argentina. Rifting started in Peru in the late Permian to early Jurassic (Ramos and Aleman 2000; Sempere et al. 2002), and reached Argentina in the Cretaceous (Viramonte et al. 1999). The main phase of rifting in Bolivia coincides with a decrease in the magmatic activity in the arc in between 120 and 80 Ma (Hammerschmidt et al. 1992). This period was characterised by a reorganisation of the oceanic plates in the eastern Pacific Ocean, and the subduction direction of

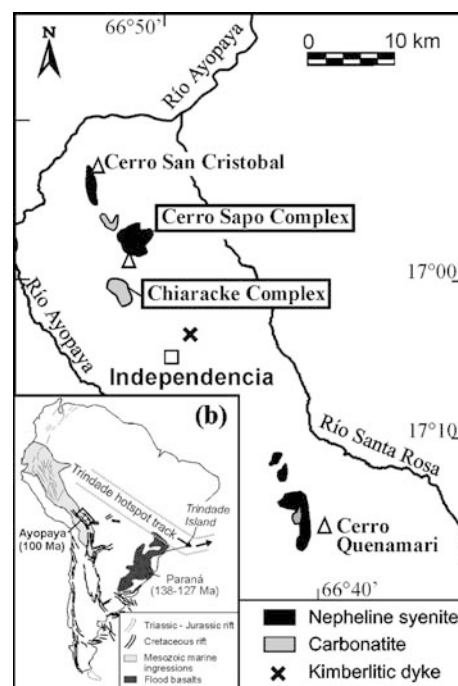


**Fig. 1** Location of major alkaline intrusive units of the Ayopaya alkaline province. Inset with sketch map of large-scale rifting of South America during the Cretaceous (compiled from Ramos and Aleman 2000; Avila Salinas 1989; Jaillard et al. 2000; Tompkins and Gonzaga 1989; Sempere et al. 1998). The intracontinental Cretaceous evolution of South America represents failed rifts on a convergent margin. During the Andean orogeny parts of the rift system, such as in Ayopaya, were inverted and eroded. The Cretaceous kimberlites and alkaline complexes of central Brazil (e.g. Alto Paranaíba, Juína) are related to mantle plume activity which presently is situated under Trindade Island (Gibson et al. 1995)

the Pacific lithosphere changed fundamentally from SE to NE (e.g. Scheuber et al. 2000).

Potassium–Argon isotope data on phlogopite megacrysts from ultramafic breccia ( $100.7 \pm 1.2$  Ma) and lamprophyre ( $99.0 \pm 1.1$  Ma) define a Cretaceous age for the magmatic rock sequence (Table 1). This is in agreement with earlier results by Kennan et al. (1995) who dated a phlogopite megacryst from the Laguna Khoallaqui, 6 km NW of Independencia (Fig. 1) at  $98 \pm 3$  Ma.

The igneous rock suite of the Ayopaya province comprises a great variety of alkaline, predominantly sodic, rocks consisting of nepheline syenite to foyaite stocks, carbonatite intrusions and dykes, ultramafic breccias and dykes of melilititic–nephelinitic composi-

**Table 1** K–Ar age data for dark mica from ultramafic breccia (I6a and AR-1) and a lamprophyre sample (I15)

Sample	Location	Sample material	K (wt %)	rad. Ar. (nl/g)	rad. Ar (%)	Age (Ma)
I 6a	Laguna Khoallaqui	Phlogopite megacryst	7.84	31.8	91.0	$100.7 \pm 1.2$
I 15	Khorí-Mayu	Biotite megacryst	7.62	30.2	92.4	$99.0 \pm 1.1$
AR-1	Laguna Khoallaqui	Phlogopite megacryst	7.87	30.7	–	$97.7 \pm 2.8$

Data on AR-1 from Kennan et al. (1995: 169). Decay constants are from Steiger and Jäger (1977)

tion and a kimberlitic dyke near the village of Independencia (Figs. 1 and 2). Small dykes and sills of basanite, tephrite, phonolite and lamprophyre are widespread in the entire Ayopaya region. The nepheline syenitic stocks of the Cerro Sapo and the Cerro San Cristobal are intimately associated with small carbonatitic intrusive bodies and dykes (Fig. 1). Additionally, the Cerro Sapo complex hosts a spectacular sodalite-ankerite-baryte dyke system (Figs. 2 and 3). In contrast to the Cerro Sapo complex the Chiaracke carbonatite intrusion shows no relation to magmatic silicate rocks.

The country rocks of the alkaline intrusions consist of very-low-grade metamorphic Ordovician to Devonian shales and sandstones (Kley et al. 1997). This more than 10-km-thick clastic sequence forms the backbone of the Eastern Andes of Bolivia.

### Analytical methods

Major and most trace elements were measured by X-ray fluorescence spectrometry on lithium metaborate fused disks at Bundesanstalt für Geowissenschaften und Rohstoffe, Hannover (Tables 2, 3 and 4). Rare-earth elements were measured by inductively-coupled plasma mass spectrometry (ICP-MS) at Bundesanstalt für Geowissenschaften und Rohstoffe, Hannover, and at GeoForschungsZentrum Potsdam. Some samples were also analysed by ICP-MS for Sc, Cs, Pb, Th and U.

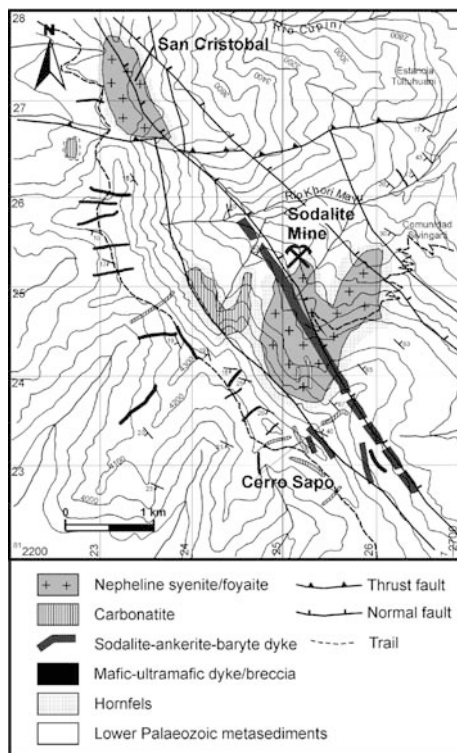


**Fig. 2** Geological map of the Cerro Sapo alkaline complex (modified after Balderrama Zárata 2003)

These data are given in three-digit numbers. The digestion of samples for ICP-MS was by HF/HClO<sub>4</sub> in Teflon beakers at 200°C and followed standard procedures. F

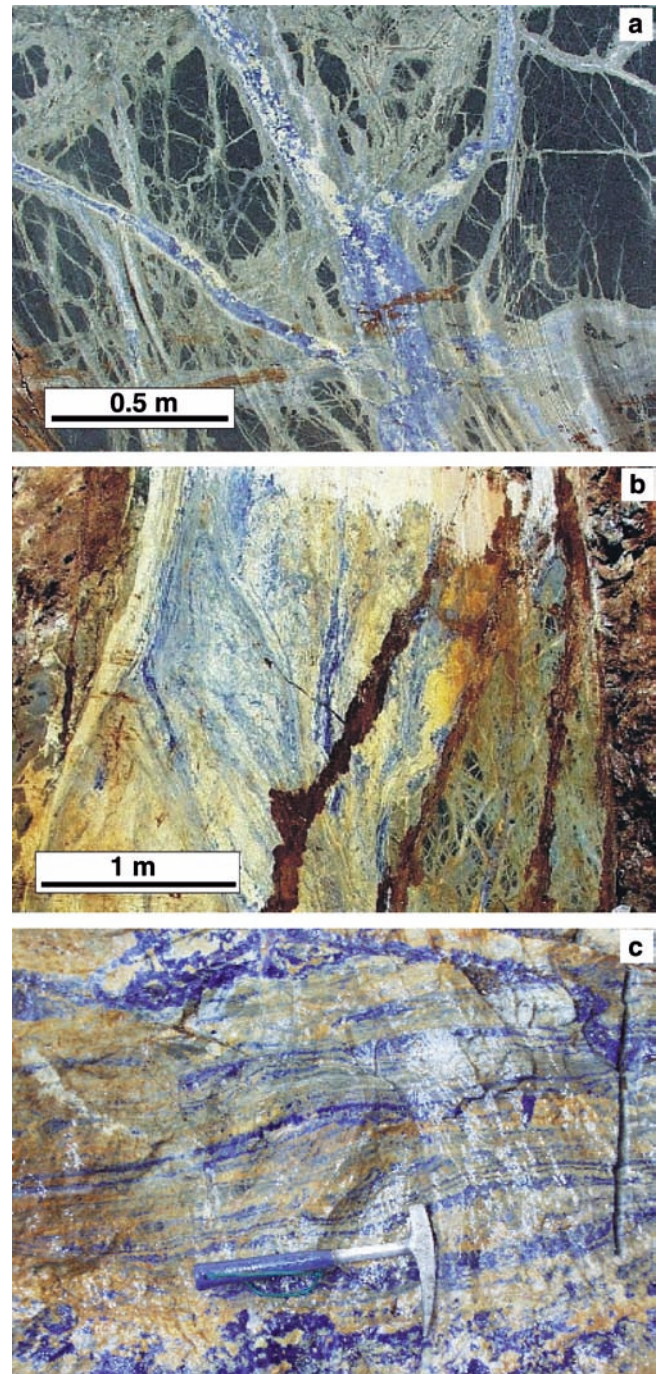


**Fig. 3** Rock textures in the sodalite-ankerite-baryte dyke. **a** Sodalite-ankerite stockwork in syenitic host rock. Veinlets of sodalite (blue) and ankerite (yellow) surrounded by narrow zones of fenitisation (greenish-grey bleached). Outcrop at the mining face of the sodalite mine in the immediate hanging wall of the sodalite-ankerite dyke. **b** Fluidal texture consisting of narrow sodalite-ankerite flow-banding in the sodalite-ankerite dyke system. Picture taken from the slope of the Cerro Sapo sodalite mine. **c** Narrow layering of sodalite (dark blue) and ankerite (yellow) indicating rhythmic crystallisation from a highly fractionated carbonated silicate system

**Table 2** Major and trace element composition of the major alkaline silicate rocks of Ayopaya

	Cerro Sapo				Cerro San Cristobal		Quenamari
	Ijolite I39	Foyaite I30	Ne syenite I44	Sodalite AY25	Hbl syenite I34	Foyaite I126	Ne syenite I46
SiO <sub>2</sub> (wt %)	44.1	53.2	52.9	37.0	55.6	56.15	44.4
TiO <sub>2</sub>	2.10	0.75	0.42	0.07	0.85	0.18	2.56
Al <sub>2</sub> O <sub>3</sub>	14.6	21.2	20.7	31.6	18.8	21.34	16.4
ΣFe <sub>2</sub> O <sub>3</sub>	11.2	4.23	3.86	0.28	6.37	2.45	10.3
MnO	0.188	0.138	0.199	0.021	0.172	0.111	0.174
MgO	8.24	0.54	0.22	0.07	2.03	0.14	4.11
CaO	10.1	2.64	1.80	0.33	3.70	0.97	7.81
Na <sub>2</sub> O	4.86	9.17	9.0	24.4	6.22	8.96	4.69
K <sub>2</sub> O	2.45	5.70	5.56	0.44	4.25	6.24	3.14
P <sub>2</sub> O <sub>5</sub>	0.46	0.12	0.06	0.04	0.27	0.06	0.92
Cl	0.100	0.342	0.956	4.55	0.104	NA	0.016
F	0.125	0.035	0.056	<0.05	0.088	NA	0.104
LOI	0.86	1.29	2.29	1.02	1.21	1.84	4.77
Total	99.4	99.3	98.0	99.7	99.6	98.4	99.4
Sc (ppm)	19	4	<2	<2	6	0.3	10
V	223	38	19	10	57	14	193
Cr	328	<3	7	7	63	6	30
Co	51	4	10	<3	18	1	44
Ni	158	<3	<3	<3	29	2	22
Cu	52	14	15	35	22	2	22
Zn	115	76	106	287	130	206	106
Ga	22	25	34	50	25	32	19
As	5	3	18	11	8	18	4
Br	NA	NA	NA	300	NA	27	NA
Rb	97	203	200	6	200	301	113
Sr	833	1,519	874	812	582	613	866
Y	24	19	47	19	27	12	26
Zr	271	304	457	<3	514	297	249
Nb	124	183	218	30	139	55	121
Mo	12	2	81	5	5	<5	14
Sn	<2	5	<2	<2	5	<2	<2
Cs	<5	<5	<5	<5	10	12.9	<5
Ba	920	1,486	610	4,426	732	849	1,115
La	67.3	27.8	199	68.0	61.8	25.7	62.4
Ce	123	59.3	255	140	124	35.8	118
Pr	13.3	6.7	NA	NA	10.5	3.0	13.1
Nd	48.3	24.5	NA	NA	33.3	8.0	49.7
Sm	8.6	4.3	NA	NA	5.4	1.1	8.91
Eu	2.5	1.3	NA	NA	1.2	0.3	2.62
Gd	7.5	3.7	NA	NA	4.7	0.87	7.88
Tb	1	0.56	NA	NA	0.73	0.14	1.05
Dy	5.5	3.1	NA	NA	4.3	0.86	5.59
Ho	0.97	0.57	NA	NA	0.83	0.17	1.00
Er	2.6	1.7	NA	NA	2.6	0.52	2.77
Tm	0.34	0.25	NA	NA	0.40	0.08	0.38
Yb	2.2	1.8	NA	NA	2.7	0.61	2.25
Lu	0.31	0.30	NA	NA	0.43	0.10	0.35
Ta	9	5	14	<5	9	4	9
W	14	<5	15	<5	8	8	9
Pb	<4	25	39	58	15	101	<4
Th	11	5	48	96	27	21	5
U	8	6	23	<3	9	7	7
(Na + K)/Al	0.73	1.03	1.03	1.10	0.82	1.05	0.70
Mg#	0.57	0.19	0.09	0.31	0.36	0.09	0.42

NA not analysed

was determined by H<sub>3</sub>PO<sub>4</sub> distillation and ion-selective electrode; CO<sub>2</sub> by colorimetric titration.

Most of the Sr and Nd isotope analyses were done at the Laboratory of Isotopic Geochronology and Geochemistry of the Institute of Precambrian Geology and Geochronology, St Petersburg, Russia (Table 5). The measurements were performed on a Finnigan MAT-261

mass spectrometer equipped with eight collectors under static mode. The <sup>143</sup>Nd/<sup>144</sup>Nd ratio was normalised within-run to <sup>148</sup>Nd/<sup>144</sup>Nd = 0.241570 and adjusted to a <sup>143</sup>Nd/<sup>144</sup>Nd value of 0.511860 for La Jolla. Repeat measurements of <sup>143</sup>Nd/<sup>144</sup>Nd ratio of the La Jolla standard varied from 0.511875 to 0.511912 with a mean value of 0.511894 ± 10 (*n* = 57). Sr isotope composition

Table 3 Major and trace element composition of the carbonatite rock suite of Ayopaya

	Chiaracke (Magnesiocarbonatite)										Dykes and lenses					Cerro Sapo				Sodalite-ankerite-baryte dyke				Cristobal [Calciocarbonatite]	Diatreme																																																																																																																																																																																																																																																																																																																																																																																																																																																																																																																																																																																																																																																																																																																																																																																																																																																																																																																																																																																																																																																																																																																																																																																																																																																																																																																																																																																																																																																																																																																																																																																																																																																																																																																																																																																																																																																																																																																																																																																																																																																																																																																																																																																																																																																																																																																																																																																																																																																																																																																																																																																																																																																																																																																																																																																																																																																																																																																																																																																																																																																																																																																																																																																																																																																																																																																																																																																																																																																																																																																																																																																																																																																																																																																																																																																																																																																																																																																																																																																																																																																																																																																																																																																																																		
	178					180					181					182					183					188					192					193					194					195					196					197					198					199					200					201					202					203					204					205					206					207					208					209					210					211					212					213					214					215					216					217					218					219					220					221					222					223					224					225					226					227					228					229					230					231					232					233					234					235					236					237					238					239					240					241					242					243					244					245					246					247					248					249					250					251					252					253					254					255					256					257					258					259					260					261					262					263					264					265					266					267					268					269					270					271					272					273					274					275					276					277					278					279					280					281					282					283					284					285					286					287					288					289					290					291					292					293					294					295					296					297					298					299					300					301					302					303					304					305					306					307					308					309					310					311					312					313					314					315					316					317					318					319					320					321					322					323					324					325					326					327					328					329					330					331					332					333					334					335					336					337					338					339					340					341					342					343					344					345					346					347					348					349					350					351					352					353					354					355					356					357					358					359					360					361					362					363					364					365					366					367					368					369					370					371					372					373					374					375					376					377					378					379					380					381					382					383					384					385					386					387					388					389					390					391					392					393					394					395					396					397					398					399					400					401					402					403					404					405					406					407					408					409					410					411					412					413					414					415					416					417					418					419					420					421					422					423					424					425					426					427					428					429					430					431					432					433					434					435					436					437					438					439					440					441					442					443					444					445					446					447					448					449					450					451					452					453					454					455					456					457					458					459					460					461					462					463					464					465					466					467					468					469					470					471					472					473					474					475					476					477					478					479					480					481					482					483					484					485					486					487					488					489					490					491					492					493					494					495					496					497					498					499					500					501					502					503					504					505					506					507					508					509					510					511					512					513					514					515					516					517					518					519					520					521					522					523					524					525					526					527					528					529					530					531					532					533					534					535					536					537					538					539					540					541					542					543					544					545					546					547					548					549					550					551					552					553					554					555					556					557					558					559					560					561					562					563					564					565					566					567					568					569					570					571					572					573					574					575					576					577					578					579					580					581					582					583					584					585					586					587					588					589					590					591					592					593					594					595					596					597					598					599					600					601					602					603					604					605					606					607					608					609					610					611					612					613					614					615					616					617					618					619					620					621					622					623					624					625					626					627					628					629					630					631					632					633					634					635					636					637					638					639					640					641					642					643					644					645					646					647					648					649					650					651					652					653					654					655					656					657					658					659					660					661					662					663					664					665					666					667					668					669					670					671					672					673					674					675					676					677					678					679					680					681					682					683					684					685					686					687					688					689					690					691					692					693					694					695					696					697					698					699					700					701					702					703					704					705					706					707					708					709					710					711					712					713					714					715					716					717					718					719					720					721					722					723					724					725					726					727					728					729					730					731					732					733					734					735					736					737					738					739					740					741					742					743					744					745					746					747					748					749					750					751					752					753					754					755					756					757					758					759					760					761					762					763					764					765					766					767					768					769					770					771					772					773					774					775					776					777					778					779					780					781					782					783					784					785					786					787					788					789					790					791					792					793					794					795					796					797					798					799					800					801					802					803					804					805					806					807					808					809					810					811					812					813					814					815					816					817					818					819					820					821					822					823					824					825					826					827					828					829					830					831					832					833					834					835					836					837					838					839					840					841					842					843					844					845					846					847					848					849					850					851					852					853					854					855					856					857					858					859					860					861					862					863					864					865					866					867					868					869					870					871					872					873					874					875					876					877					878					879					880					881					882					883					884					885					886					887					888					889					890					891					892					893					894					895					896					897					898					899					900					901					902					903					904					905					906					907					908					909					910					911					912					913					914					915					916					917					918					919					920					921					922					923					924					925					926					927					928					929					930					931					932					933					934					935					936					937					938					939					940					941					942					943					944					945					946					947					948					949					950					951					952					953					954					955					956					957					958					959					960					961					962					963					964					965					966					967					968					969					970					971					972					973					974					975					976					977					978					979					980					981					982					983					984					985					986					987					988					989					990					991					992					993					994					995					996					997					998					999					1000				
	SiO <sub>2</sub> (wt %)	2.27	0.14	0.70	0.07	0.71	<0.1	0.54	8.75	13.7	6.44	0.30	2.16	1.25	15.8	23.2	12.9	1.36	4.98																																																																																																																																																																																																																																																																																																																																																																																																																																																																																																																																																																																																																																																																																																																																																																																																																																																																																																																																																																																																																																																																																																																																																																																																																																																																																																																																																																																																																																																																																																																																																																																																																																																																																																																																																																																																																																																																																																																																																																																																																																																																																																																																																																																																																																																																																																																																																																																																																																																																																																																																																																																																																																																																																																																																																																																																																																																																																																																																																																																																																																																																																																																																																																																																																																																																																																																																																																																																																																																																																																																																																																																																																																																																																																																																																																																																																																																																																																																																																																																																																																																																																																																																																																																																																								
TiO <sub>2</sub>	0.006	0.004	0.007	0.007	0.007	0.017	0.003	0.168	0.199	0.663	0.042	0.143	0.016	0.002	<0.001	0.010	0.015	1.38																																																																																																																																																																																																																																																																																																																																																																																																																																																																																																																																																																																																																																																																																																																																																																																																																																																																																																																																																																																																																																																																																																																																																																																																																																																																																																																																																																																																																																																																																																																																																																																																																																																																																																																																																																																																																																																																																																																																																																																																																																																																																																																																																																																																																																																																																																																																																																																																																																																																																																																																																																																																																																																																																																																																																																																																																																																																																																																																																																																																																																																																																																																																																																																																																																																																																																																																																																																																																																																																																																																																																																																																																																																																																																																																																																																																																																																																																																																																																																																																																																																																																																																																																																																																																									
Al <sub>2</sub> O <sub>3</sub>	0.14	<0.05	<0.05	<0.05	0.47	0.06	<0.05	2.63	4.04	1.84	0.10	0.13	<0.05	10.9	10.4	11.5	0.33	1.37																																																																																																																																																																																																																																																																																																																																																																																																																																																																																																																																																																																																																																																																																																																																																																																																																																																																																																																																																																																																																																																																																																																																																																																																																																																																																																																																																																																																																																																																																																																																																																																																																																																																																																																																																																																																																																																																																																																																																																																																																																																																																																																																																																																																																																																																																																																																																																																																																																																																																																																																																																																																																																																																																																																																																																																																																																																																																																																																																																																																																																																																																																																																																																																																																																																																																																																																																																																																																																																																																																																																																																																																																																																																																																																																																																																																																																																																																																																																																																																																																																																																																																																																																																																																																									
ΣFe <sub>2</sub> O <sub>3</sub>	9.9	8.8	24.1	1.61	12.4	6.04	9.3	42.8	13.7	14.6	3.41	4.22	3.52	14.0	11.7	12.7	3.75	19.3																																																																																																																																																																																																																																																																																																																																																																																																																																																																																																																																																																																																																																																																																																																																																																																																																																																																																																																																																																																																																																																																																																																																																																																																																																																																																																																																																																																																																																																																																																																																																																																																																																																																																																																																																																																																																																																																																																																																																																																																																																																																																																																																																																																																																																																																																																																																																																																																																																																																																																																																																																																																																																																																																																																																																																																																																																																																																																																																																																																																																																																																																																																																																																																																																																																																																																																																																																																																																																																																																																																																																																																																																																																																																																																																																																																																																																																																																																																																																																																																																																																																																																																																																																																																																									
MnO	2.20	1.60	2.94	2.06	1.61	1.05	2.17	4.52	2.53	2.02	0.915	0.812	0.231	1.12	0.919	0.997	0.772	0.991																																																																																																																																																																																																																																																																																																																																																																																																																																																																																																																																																																																																																																																																																																																																																																																																																																																																																																																																																																																																																																																																																																																																																																																																																																																																																																																																																																																																																																																																																																																																																																																																																																																																																																																																																																																																																																																																																																																																																																																																																																																																																																																																																																																																																																																																																																																																																																																																																																																																																																																																																																																																																																																																																																																																																																																																																																																																																																																																																																																																																																																																																																																																																																																																																																																																																																																																																																																																																																																																																																																																																																																																																																																																																																																																																																																																																																																																																																																																																																																																																																																																																																																																																																																																																									
MgO	23.6	17.0	20.6	4.96	16.6	17.3	14.8	5.87	7.49	6.18	0.71	1.13	0.25	4.00	3.43	4.07	0.48	7.25																																																																																																																																																																																																																																																																																																																																																																																																																																																																																																																																																																																																																																																																																																																																																																																																																																																																																																																																																																																																																																																																																																																																																																																																																																																																																																																																																																																																																																																																																																																																																																																																																																																																																																																																																																																																																																																																																																																																																																																																																																																																																																																																																																																																																																																																																																																																																																																																																																																																																																																																																																																																																																																																																																																																																																																																																																																																																																																																																																																																																																																																																																																																																																																																																																																																																																																																																																																																																																																																																																																																																																																																																																																																																																																																																																																																																																																																																																																																																																																																																																																																																																																																																																																																																									
CaO	17.1	27.3	4.96	19.1	28.7	28.8	28.8	10.9	21.3	23.2	48.3	47.1	51.1	16.5	12.9	15.9	49.1	25.0																																																																																																																																																																																																																																																																																																																																																																																																																																																																																																																																																																																																																																																																																																																																																																																																																																																																																																																																																																																																																																																																																																																																																																																																																																																																																																																																																																																																																																																																																																																																																																																																																																																																																																																																																																																																																																																																																																																																																																																																																																																																																																																																																																																																																																																																																																																																																																																																																																																																																																																																																																																																																																																																																																																																																																																																																																																																																																																																																																																																																																																																																																																																																																																																																																																																																																																																																																																																																																																																																																																																																																																																																																																																																																																																																																																																																																																																																																																																																																																																																																																																																																																																																																																																																									
Na <sub>2</sub> O	0.06	0.02	0.08	0.1	<0.01	<0.01	0.03	0.08	0.51	0.14	0.11	0.65	0.20	4.35	6.24	8.34	0.07	0.15																																																																																																																																																																																																																																																																																																																																																																																																																																																																																																																																																																																																																																																																																																																																																																																																																																																																																																																																																																																																																																																																																																																																																																																																																																																																																																																																																																																																																																																																																																																																																																																																																																																																																																																																																																																																																																																																																																																																																																																																																																																																																																																																																																																																																																																																																																																																																																																																																																																																																																																																																																																																																																																																																																																																																																																																																																																																																																																																																																																																																																																																																																																																																																																																																																																																																																																																																																																																																																																																																																																																																																																																																																																																																																																																																																																																																																																																																																																																																																																																																																																																																																																																																																																																																									
K <sub>2</sub> O	0.16	0.03	0.03	0.08	0.08	0.01	0.04	1.93	2.41	1.39	0.03	0.06	0.08	0.18	0.07	0.17	0.19	0.89																																																																																																																																																																																																																																																																																																																																																																																																																																																																																																																																																																																																																																																																																																																																																																																																																																																																																																																																																																																																																																																																																																																																																																																																																																																																																																																																																																																																																																																																																																																																																																																																																																																																																																																																																																																																																																																																																																																																																																																																																																																																																																																																																																																																																																																																																																																																																																																																																																																																																																																																																																																																																																																																																																																																																																																																																																																																																																																																																																																																																																																																																																																																																																																																																																																																																																																																																																																																																																																																																																																																																																																																																																																																																																																																																																																																																																																																																																																																																																																																																																																																																																																																																																																																																									
P <sub>2</sub> O <sub>5</sub>	0.431	0.012	1.03	2.81	2.81	0.757	0.079	0.904	0.107	0.073	1.30	0.329	3.22	0.180	0.030	0.290	0.099	0.068																																																																																																																																																																																																																																																																																																																																																																																																																																																																																																																																																																																																																																																																																																																																																																																																																																																																																																																																																																																																																																																																																																																																																																																																																																																																																																																																																																																																																																																																																																																																																																																																																																																																																																																																																																																																																																																																																																																																																																																																																																																																																																																																																																																																																																																																																																																																																																																																																																																																																																																																																																																																																																																																																																																																																																																																																																																																																																																																																																																																																																																																																																																																																																																																																																																																																																																																																																																																																																																																																																																																																																																																																																																																																																																																																																																																																																																																																																																																																																																																																																																																																																																																																																																																																									
CO <sub>2</sub>	40.9	44.1	37.8	36.8	44.7	43.5	19.2	32.5	32.8	32.9	41.0	40.7	38.3	27.1	23.4	27.5	41.1	35.7																																																																																																																																																																																																																																																																																																																																																																																																																																																																																																																																																																																																																																																																																																																																																																																																																																																																																																																																																																																																																																																																																																																																																																																																																																																																																																																																																																																																																																																																																																																																																																																																																																																																																																																																																																																																																																																																																																																																																																																																																																																																																																																																																																																																																																																																																																																																																																																																																																																																																																																																																																																																																																																																																																																																																																																																																																																																																																																																																																																																																																																																																																																																																																																																																																																																																																																																																																																																																																																																																																																																																																																																																																																																																																																																																																																																																																																																																																																																																																																																																																																																																																																																																																																																																									
F	1.33	0.113	0.267	0.721	0.189	0.189	0.505	0.085	0.055	0.269	0.133	0.140	0.317	0.155	n.a.	n.a.	0.083	0.118																																																																																																																																																																																																																																																																																																																																																																																																																																																																																																																																																																																																																																																																																																																																																																																																																																																																																																																																																																																																																																																																																																																																																																																																																																																																																																																																																																																																																																																																																																																																																																																																																																																																																																																																																																																																																																																																																																																																																																																																																																																																																																																																																																																																																																																																																																																																																																																																																																																																																																																																																																																																																																																																																																																																																																																																																																																																																																																																																																																																																																																																																																																																																																																																																																																																																																																																																																																																																																																																																																																																																																																																																																																																																																																																																																																																																																																																																																																																																																																																																																																																																																																																																																																																																									
SO <sub>3</sub>	0.47	0.05	2.52	2.95	2.95	0.07	0.51	2.38	0.85	2.26	0.28	1.86	2.68																																																																																																																																																																																																																																																																																																																																																																																																																																																																																																																																																																																																																																																																																																																																																																																																																																																																																																																																																																																																																																																																																																																																																																																																																																																																																																																																																																																																																																																																																																																																																																																																																																																																																																																																																																																																																																																																																																																																																																																																																																																																																																																																																																																																																																																																																																																																																																																																																																																																																																																																																																																																																																																																																																																																																																																																																																																																																																																																																																																																																																																																																																																																																																																																																																																																																																																																																																																																																																																																																																																																																																																																																																																																																																																																																																																																																																																																																																																																																																																																																																																																																																																																																																																																																														

Table 3 (Contd.)

	Chiaracke (Magnesiocarbonatite)										Cerro Sapo				Cristobal [Calciocarbonatite]		Diatreme		
	Dykes and lenses					Dykes and lenses					Calciocarbonatite		Sodalite-ankerite-baryte dyke					I127b	I70a
	I174	I178	I179	I180	I181	I182	I183	I22	I23	I23	I123	I140	I153a	I162	AY24	AY11			
Yb	2.61	1.80	1.95	4.10	2.5	5.61	2.35	5.01	1.89	3.5	14.2	7.65	1.91	9.30	2.10	2.40	5.38		
Lu	0.55	0.38	0.69	-	0.40	0.69	-	0.71	0.38	-	1.99	1.02	0.30	1.20	0.20	0.30	0.81		
Ta	<1	<1	<1	<1	<1	<1	<1	8	<5	<1	<5	<1	8	<1	<1	<1	<1		
Pb	18	18	10	7	34	7	111	560	300	1,620	11	35	14	2,645	19	56	48		
Th	240	277	405	817	600	30	323	405	433	6,040	<5	34.4	1.5	2,033	1,440	1,380	26.4		
U	3.52	0.04	0.12	0.41	0.55	0.16	0.01	3	<3	<3	5.00	1.31	1.44	0.6	0.8	0.9	6.33		
Ca#	0.46	0.66	0.22	0.58	0.66	0.70	0.69	0.81	0.77	0.82	0.99	0.98	1.00	0.83	0.82	0.82	0.99		
Mg#	0.81	0.78	0.60	0.70	0.84	0.74	0.20	0.44	0.49	0.43	0.27	0.32	0.11	0.34	0.34	0.36	0.19		

Low totals in the sodalite-ankerite dyke are due to high chlorine content (not analysed) and high trace element contents (e.g. Sr, Ba).  
N/A not analysed

was normalised within-run to  $^{88}\text{Sr}/^{86}\text{Sr} = 8.37521$ . The value of Sr isotope standard SRM-987 during this work was  $^{87}\text{Sr}/^{86}\text{Sr} = 0.710248 \pm 15$  ( $2\sigma$ , 16 runs). Assigned errors ( $2\sigma$ ) for  $^{147}\text{Sm}/^{144}\text{Nd}$  and  $^{143}\text{Nd}/^{144}\text{Nd}$  were  $\pm 0.3$  and  $\pm 0.000015\%$ ,  $^{87}\text{Rb}/^{86}\text{Sr} \pm 0.5$ ,  $^{87}\text{Sr}/^{86}\text{Sr} \pm 0.000025\%$  according to results of multiple standard analyses (external reproducibility). The  $2\sigma$  errors cited in Table 5 for  $^{143}\text{Nd}/^{144}\text{Nd}$  and  $^{87}\text{Sr}/^{86}\text{Sr}$  reflect in-run precision. The blank level was 0.01 ng for Sm and 0.05 ng for Nd, 0.05 ng for Rb and 0.2 ng for Sr. The data obtained for the BCR-1 standard are: [Sr] = 335.8 ppm, [Rb] = 47.16 ppm, [Sm] = 6.487 ppm, [Nd] = 28.45 ppm,  $^{87}\text{Sr}/^{86}\text{Sr} = 0.705053 \pm 11$ ,  $^{87}\text{Rb}/^{86}\text{Sr} = 0.40615$ ,  $^{143}\text{Nd}/^{144}\text{Nd} = 0.512663 \pm 9$ ,  $^{147}\text{Sm}/^{144}\text{Nd} = 0.13829$ . Some samples were analysed for Sr- and Nd-isotope ratios by the radiogenic isotope lab of Bundesanstalt für Geowissenschaften und Rohstoffe, Hannover, Germany. The error estimate for  $^{147}\text{Sm}/^{144}\text{Nd}$  is  $\pm 0.01\%$  ( $2\sigma$ ), for  $^{147}\text{Sm}/^{144}\text{Nd} \pm 1\%$ . La Jolla  $^{143}\text{Nd}/^{144}\text{Nd}$  standard:  $0.511844 \pm 15$  ( $2\sigma$ ).

Reconnaissance oxygen and carbon isotope analysis on ten whole-rock samples was done by the stable isotope lab of the University of Göttingen (Prof. Hoefs). The sample powder was treated with 100% phosphoric acid, and the liberated  $\text{CO}_2$  was measured with a Finnigan MAT 251 mass spectrometer. The results of the oxygen and carbon isotope analyses are given in the usual permil deviation relative to SMOW and PDB, respectively (Table 6). The reproducibility of both  $\delta$  values is better than  $\pm 0.2\%$ . Potassium-argon dating of two dark mica concentrates was by the isotope lab of Bundesanstalt für Geowissenschaften und Rohstoffe (Table 1). Argon was measured by isotope dilution with a mean standard deviation of 0.75% ( $2\sigma$ ). Optical petrography was accompanied by qualitative electron microprobe analysis by a Cameca SX 100 at Technical University of Clausthal.

## Petrology

In the following section we will give an overview of the petrography and geochemistry of the major igneous rocks of the Ayopaya alkaline province, with focus on the Cerro Sapo complex and the Chiaracke intrusion.

### Cerro Sapo alkaline complex

The Cerro Sapo intrusion (Fig. 2) consists predominantly of biotite-clinopyroxene-nepheline syenite/foyaite and sodalite-orthoclase foyaite/syenite with minor ijolite. The mineral assemblage comprises micropertthitic orthoclase, nepheline, sodalite, clinopyroxene, plagioclase, biotite, barkevikite, natrolite, cancrinite and apatite. The clinopyroxene is diopside with aegirine-augite rims. Sodalite is ubiquitous and represents the latest magmatic mineral phase. Sodalite is a rare foid-mineral that is characterised by unusually high  $\text{Na}_2\text{O}$  (up to





**Table 6** Carbon and oxygen isotopic composition of carbonatite samples from Ayopaya

Sample	Rock	$\delta^{13}\text{C}_{\text{PDB}}$	$\delta^{18}\text{O}_{\text{SMOW}}$
I5	Ferrocarnatite	-4.68	12.6
I22	Ferrocarnatite	-4.72	14.0
I40	Calciocarnatite	-9.18	10.9
I62	Calciocarnatite	-7.67	7.16
I53a	Calciocarnatite	-8.64	10.3
I53b	Calciocarnatite	-8.08	11.0
I70a	Ferrocarnatite	-5.37	14.3
I78	Magnesiocarnatite	-4.94	11.9
I81	Magnesiocarnatite	-5.70	12.3
I82	Magnesiocarnatite	-6.16	12.1

25 wt%) and Cl (up to 5 wt%) contents. The rocks are highly alkaline to peralkaline (Table 2). Most samples have  $(\text{Na}_2\text{O}-2) > \text{K}_2\text{O}$  indicating a highly sodic character (Le Bas et al. 1986).

A small calciocarnatitic intrusive body occurs in the sedimentary host rock north-west of the nepheline-syenitic stock (Fig. 2). The body is accompanied by a network of calciocarnatitic to ferrocarnatitic dykes and dykelets and has a surface expression of 300 by 900 m (Balderrama Zàrate 2003). The thickness of the dykes ranges from a few centimetre to several metre. Calciocarnatitic dykes have also been found inside the syenitic stock. Ahlfeld and Mosebach (1935) found large boulders (up to 10 m) of white carbonatite in the Khori Mayu river in the immediate vicinity of the syenitic stock and described them first as "marbles", later reinterpreted as possible carbonatites (Ahlfeld 1966). The rocks represent nearly pure equigranular anhedral to subhedral calciocarnatite with smaller patches of ferruginous silicocarnatites (Fig. 4). Ahlfeld and Mosebach (1935) also reported on abundant purple fluorite layers. The mineral association of these carbonatites comprises predominantly calcite with minor amounts of stron-

tianite, apatite, Sr- and REE-rich hydroxylcarbonates (ancylite group) and fluorcarbonates (synchysite group), baryte, pyrite, sphalerite, amphibole, pyrochlore, diopside, and mica. Small ferrocarnatitic dykes in the sedimentary host rock are associated with the calciocarnatite intrusion, and contain synchysite/parisite, minor churchite (Dy-Gd-phosphate), and an exotic Th-rich mineralisation with thorite and thorbastnaesite.

Typical of all calciocarnatite dykes is the intense narrow layering parallel to the contact planes, which likely represents a fluidal texture (flow banding). The banding is characterised by layers of pyrochlore, strontianite, apatite, fluorite, amphibole and pyrite. Geochemically, the calciocarnatites (Table 3) are characterised by low silica content ( $< 2.2$  wt%  $\text{SiO}_2$ ) and low content of alkalis ( $< 1$  wt%  $\text{Na}_2\text{O} + \text{K}_2\text{O}$ ). They represent nearly pure carbonate rocks with  $\text{CaCO}_3 > 87$ wt%. The calciocarnatites show variable degree of REE enrichment and a relatively smooth REE distribution pattern similar to the intrusive silicate rocks of the Cerro Sapo area (Fig. 5). In contrast, the sodalite-ankerite-baryte dyke displays strong enrichment in the MREEs. The calciocarnatites are strongly enriched in Sr (up to 4 wt%) and Nb (up to 2,000 ppm). The thorium content of a small ferrocarnatitic dyke (Table 3: I123) reaches 6,400 ppm Th.

The nepheline-syenitic stock and the sedimentary host rock of the Cerro Sapo complex are cross-cut by a NW-SE trending sodalite-ankerite-baryte dyke (Fig. 2). The dyke has a length of more than 3 km and is up to 8 m thick. It consists of large irregular patches or bands of dark-blue sodalite changing rapidly with white-to-yellow ankerite and white baryte. This dyke is currently mined as semi-precious stone and ornamental rock.

The sodalite-ankerite-baryte dyke shows a fascinating textural variety comprising rhythmic layering and

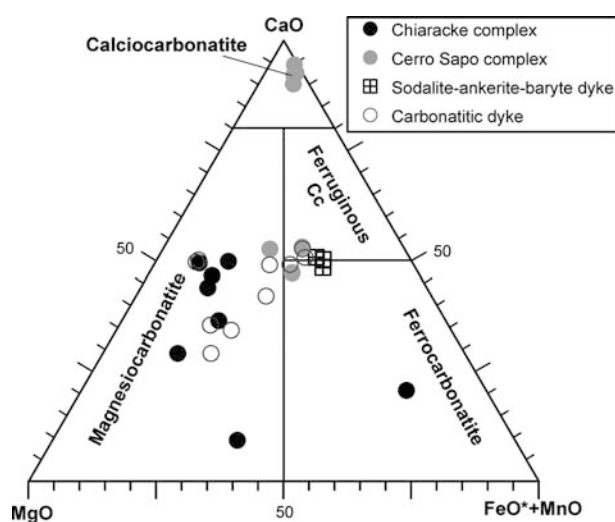


**Fig. 4** Carbonatite samples from the Ayopaya alkaline province in the revised classification diagram of Gittins and Harmer (1997); data plotted in molar proportions

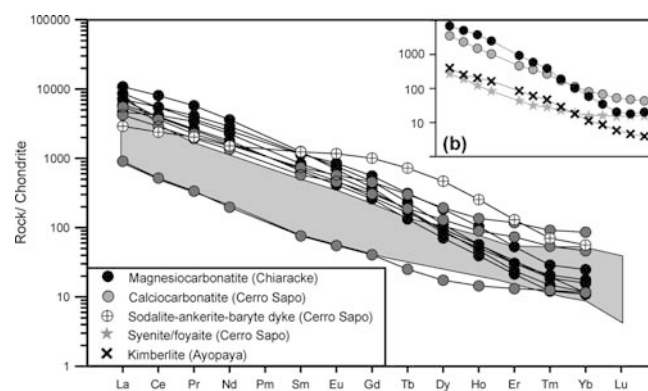


**Fig. 5** REE distribution patterns for calcio- and magnesiocarnatite samples from the Cerro Sapo and Chiaracke complexes, respectively, and a representative sample (AY24) from the sodalite-ankerite-baryte dyke at Cerro Sapo. The grey shaded field shows the composition of worldwide carbonatite occurrences compiled by Hornig-Kjarsgaard (1998). Normalising values from Evensen et al. (1978). Inset (b) shows average composition of magnesiocarnatite and calciocarnatite samples compared to the kimberlite dyke (sample I1) and average syenite/foyaite from Ayopaya

fluidal flow textures (e.g. marble cake texture) (Fig. 3). Nearly monomineralic sodalite patches in the dyke have several metres in diameter and are subhedral-granular textured. Some euhedral sodalite crystals reach up to 9 cm in size and can be described as pegmatitic. The dyke shows a very sharp intrusive contact to the magmatic nepheline-syenitic host rocks (Fig. 3). The contact zone in the syenitic host rock is brecciated and displays an intense sodalite-ankerite stockwork, with narrow zones of fenitisation (Fig. 3). Due to the strong textural and compositional heterogeneity the contribution of the main components to the dyke can only be estimated at about 40–45% sodalite, 40–45% ankerite, 10–12% baryte. Siderite, calcite, natrolite, analcime occur in minor amounts. Locally, patches and veinlets of galeinite, sphalerite, pyrite and chalcopyrite occur within the dyke. Ahlfeld and Mosebach (1935) also reported native gold in strongly weathered parts. Sodalite-rich parts of the dyke contain micro-crystal nests and veinlets of alkali-feldspar, nepheline, diopside and amphibole.

The ankerite, and sometimes also the sodalite component, contains strontium-, thorium- and REE-rich minerals such as strontianite, Sr-apatite, daqingshanite, REE-bearing strontianite, minerals of the crandallite group (goyazite), hydroxylcarbonates (mckelveyite), and Sr-rich zeolites (bellbergite). The mineral assemblage is reflected by high bulk-rock REE contents ( $\Sigma$  REE up to 0.45 wt%) and up to 2,000 ppm Th. Remarkable is the occurrence of REE-rich Sr-carbonates which contain very high amounts of thorium (1.5–10 wt% ThO<sub>2</sub>).

#### Chiaracke carbonatite intrusion

The Chiaracke intrusion, discovered by Matos (2000), is exposed about 5 km southwest of the Cerro Sapo at 4,100 m a.s.l. over an area of about 1×2 km (Fig. 1). The Chiaracke complex represents a magnesiocarbonatitic intrusion which is accompanied by many small dykes and m-sized lens-shaped bodies (1–3 m wide) of ferro-carbonatitic to silicocarbonatitic composition as well as carbonate-rich phlogopite breccias occurring widespread in the Ordovician sedimentary host rock. The carbonatite body consists of white-brown to brown coloured rocks, often showing an intense dark-brown layering. Secondary hydrothermal veinlets are characterised by purple-coloured fluorite. The mineral association of the Chiaracke intrusion comprises predominantly dolomite (Fig. 4) but also ankerite, magnesite, calcite, fluorite, strontianite, bastnaesite, monazite, apatite, potassic feldspar and magnetite.

Bastnaesite-(Ce) and monazite occur dispersed and on fissures and micro-veinlets in the carbonatite. Monazite veinlets are often associated with apatite and baryte. REE minerals of the crandallite group (florentite–goyazite) occur on veinlets together with baryte and purple-coloured fluorite. The ferrocarbonatitic to silicocarbonatitic dykes and lens-shaped bodies are characterised by small nests and veinlets of feldspar and

apatite, and sometimes large mica megacrysts up to several centimetre in size.

The magnesiocarbonatite is characterised by low silica content (mostly < 1 wt% SiO<sub>2</sub>) and low alkali content (< 0.25 wt% Na<sub>2</sub>O + K<sub>2</sub>O), and strong enrichment in LREEs (up to 3,800 ppm La, 6,600 ppm Ce, 2,100 ppm Nd, 250 ppm Sm) (Table 3) with steep REE patterns (La/Yb from 580 to 1,500) (Fig. 5). Compared to the calciocarbonatite of the Cerro Sapo the magnesiocarbonatite shows relatively low concentrations of niobium (10–170 ppm Nb), zirconium (mostly below 100 ppm Zr), and sometimes strontium, but higher contents in barium (up to 10 wt% Ba) and thorium (> 200 ppm Th) (Fig. 6).

#### Melilititic to nephelinitic dykes and diatremes

The ultramafic diatremes in the Khoallaqui (Laguna Khoallaqui) area, about 10 km N of Independencia, were the first targets of diamond exploration in the Ayopaya province. Due to their close textural similarity they have first been interpreted as kimberlitic pipes (Matos 1990). Based on petrography and geochemistry, however, they classify as melilititic to nephelinitic rocks (e.g. Fig. 7) (Lehmann and Schultz 1999).

Melilititic to nephelinitic dykes and diatremes occur widespread in the entire Ayopaya region as pale- to dark-grey fine-grained to aphanitic rocks in the sedimentary host rock. The diatremes have round to elongated shape of 10–100 m in size and are accompanied, respectively cut, by phonolitic to tephritic rocks which occur as late-stage dykes or rims around the diatremes. The diatreme rocks are dark-grey to greenish or brown and have autolithic clasts, pelletal lapilli, xenoliths and a complex suite of mega- and macrocrysts in a very heterogeneous groundmass. The

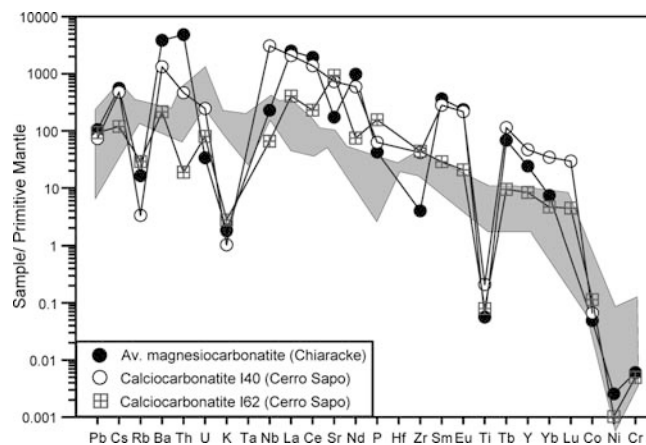
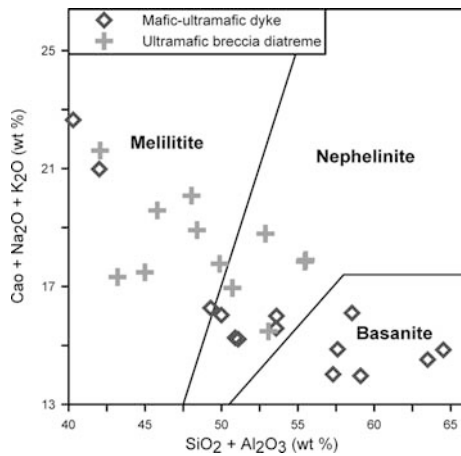


Fig. 6 Average trace-element abundances of magnesiocarbonatite from Chiaracke compared with calciocarbonatite from the Cerro Sapo, normalised to primitive mantle (after McDonough and Sun 1995). Grey shaded field is composition of nepheline syenite/foyaite



**Fig. 7** Ultramafic breccias and dykes from Ayopaya in the combined oxides diagram for discrimination between melilitite, nephelinite and basanite after Le Bas (1989)

mega- and macrocryst suite consists of different populations of forsteritic olivine and minor amounts of clinopyroxene (augite to diopside) and phlogopite. The olivine population comprises rounded mega- to macrocrysts (Mg# 0.78–0.89) but also skeletal olivine phenocrysts (“hoppers”), including “unusual hoppers” (after Moore and Erlank 1979), i.e. olivine with Mg-rich rims and Fe-rich cores. Further macrocrysts are melanite, nepheline, sodalite, chromite, perovskite, ilmenite, magnetite, pyrite and apatite. Fragments of orthoclase, sodalite and aegirine-augite are probably derived from nepheline syenite. The very heterogeneous groundmass of the dykes and diatremes comprises microlithic phlogopite, serpentine, perovskite, chromite, clinopyroxene, carbonate, apatite and glass. Zeolite pseudomorphs after lath-like melilitite microcrystals are visible in some dykes. The pseudomorphs are fluidal-textured and show the typical peg-structure. They indicate a primary melilitite content of up to 40%. Primary carbonate occurs as groundmass mineral as well as carbonatitic patches and lenses of m-size in the diatremes.

The predominantly melilititic to nephelinitic character of the dykes and diatremes (Fig. 7) is also indicated by normative larnite contents from 2 to 15% (see Woolley et al. 1996). Compared with kimberlites they are rich in Na<sub>2</sub>O and Al<sub>2</sub>O<sub>3</sub> and poor in MgO (Mg# between 0.67 and 0.72). Some of the samples can be classified as peralkaline (Table 4). The dykes and diatremes predominantly represent silica-undersaturated rocks with average titanium contents of 2.4 wt% TiO<sub>2</sub>.

Besides fragments from the sedimentary and igneous host rocks, the xenolith association of the melilititic to nephelinitic diatremes and dykes also comprises samples from the basement (gneisses) and upper mantle (lherzolitic peridotite, wehrlite, clinopyroxenite). The clinopyroxenite xenoliths are 0.5–8 cm in diameter and are rounded to weakly angular. The texture of the xenoliths is variable ranging from granular to porphyroclastic. They consist of different types of clinopyroxene,

together with amphibole, phlogopite, apatite, carbonate, titanomagnetite, melanite, sphene, and rare feldspar. The anhedral to subhedral pyroxenes are pale-green to dark-green and sometimes irregularly patchy zoned. Apatite occurs in veinlets but also intergranular between clinopyroxene crystals. Large euhedral apatite laths (> 1 cm), crosscutting the crystal faces of clinopyroxene, are probably of secondary origin.

#### Kimberlitic dyke

About 4 km NE of Independencia, a strongly weathered, dark-grey, carbonate-serpentine-rich kimberlitic dyke occurs in Ordovician shale (Fig. 1) at nearly 3,000 m a.s.l. The steeply dipping dyke has a length of about 300 m and a thickness of a few metres. The dyke has a porphyritic texture with white to light-greenish, rounded phenocrysts (0.2–0.6 cm in size) and hypidiomorphic dark phenocrysts (1–3 mm in size) set in a fine-grained dark-grey to greenish-grey groundmass. The phenocrysts constitute 25–30% of the rock. They are completely replaced by carbonate (white) and serpentine (dark) in variable proportions, with chrysotile along cleavage planes. Relics of phlogopite (up to several millimetre large) are mostly replaced by brown hydro-mica (Fig. 8). The groundmass consists of calcite pseudomorphs of olivine (?) and serpentine. Accessory mineral phases of the groundmass are chromite, perovskite, monazite, apatite, magnesite, magnetite, monticellite, pyrite and rutile.

In spite of advanced weathering and alteration, the geochemical features of this rock clearly indicate a kimberlitic composition (Table 4). This rock has the highest MgO content of all silicate rocks of the Ayopaya region with more than 22 wt% MgO and a high Mg# number of 0.79 (Table 4). Archetype kimberlites are characterised by MgO values of 25–30 wt% (Mitchell 1986), and the slightly lower value of the Ayopaya samples may be caused by the distinctive carbonatisation. High CO<sub>2</sub>-contents (up to 16 wt%) are also typical of hypabyssal kimberlites (Clement 1982). The high content of chromium (1481 ppm Cr) and nickel (1058 ppm Ni) and the steep REE distribution pattern are diagnostic for kimberlite (Fig. 9). Particularly the strong enrichment of light REE, and the strong REE fractionation (La/Yb=103) exclude a cumulate origin. The trace element pattern of the kimberlite is very similar to that of average Group I kimberlite (Fig. 9).

Kimberlitic dykes typically occur in the roots of kimberlite pipes, where they form vertically dipping tabular bodies of 1–3 m thickness (maximum 10 m) (Clement et al. 1973; Mitchell 1986). Given the relatively deep exposure level of the dyke at 3,000 m a.s.l., the diatreme-facies of the kimberlite system is likely to be eroded, whereas the melilititic diatremes at Laguna Khoallaqui, which occur at an altitude of about 4,000 m a.s.l., are still preserved.

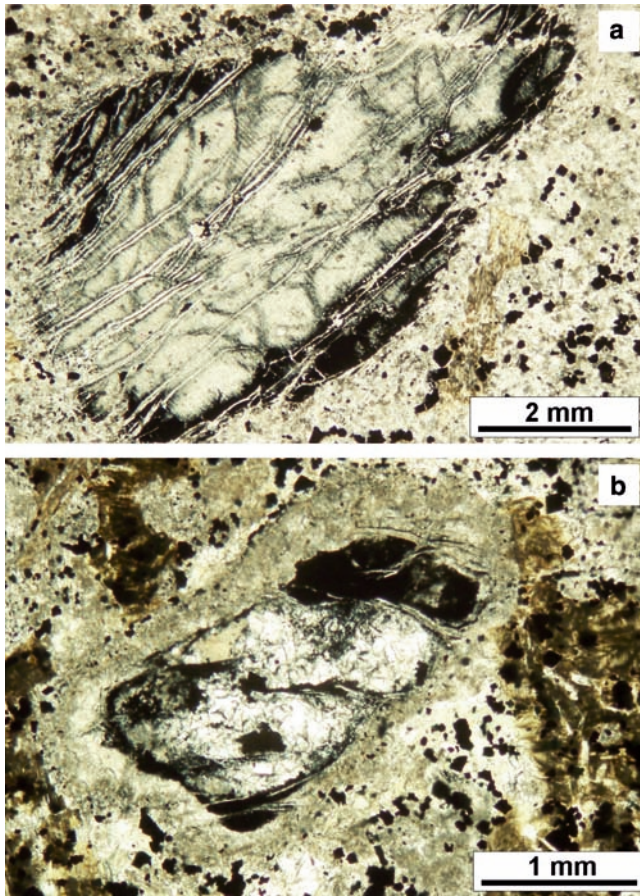


**Fig. 8** **a** Serpentinised phenocryst of olivine with chrysotile on cleavage planes and rim of opaque minerals. **b** Pseudomorphic calcite and serpentine after anhedral-rounded olivine xenocryst in fine-grained carbonate-serpentine groundmass with opaque phases (chromite, magnetite)

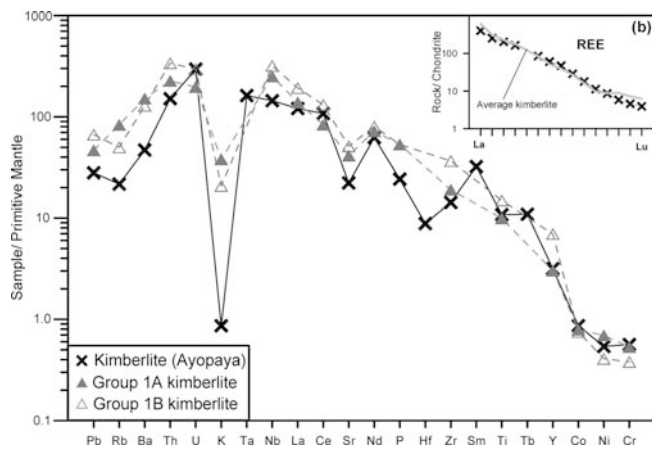


**Fig. 9** Trace-element data of the kimberlite dyke compared with average Group IA and Group IB South African kimberlites (after Smith et al. 1985). Potassium depletion of the kimberlite sample is due to alteration. Data normalised against primitive mantle (after McDonough and Sun 1995). **b** Comparison of the REE pattern of the kimberlite sample from Ayopaya with average kimberlite (grey line) according to Bergman (1987) (chondrite values from Evensen 1978)

## Discussion

Nd and Sr isotope constraints on the origin of the alkaline rock spectrum

Rb–Sr and Sm–Nd isotope data are listed in Table 5 and plotted in Fig. 10 for  $t = 100$  Ma. The alkaline rock suite from Ayopaya (carbonatite, nepheline syenite, foyaite, melilitite, nephelinite, kimberlite) shows positive  $\epsilon_{\text{Nd}}$  values of 1.4–5.4 indicating a depleted mantle source. The Chiaracke magnesiocarbonatite has high to very high  $\epsilon_{\text{Nd}}$  values together with relatively high  $^{87}\text{Sr}/^{86}\text{Sr}$  ratios. The  $^{87}\text{Sr}/^{86}\text{Sr}$  range of the magnesiocarbonatite, particularly the most radiogenic value ( $^{87}\text{Sr}/^{86}\text{Sr} = 0.70620$ ), can be attributed to hydrothermal overprint. Calcite veinlets are widespread both within and around the Chiaracke complex.

The two carbonate–phlogopite kimberlite samples have initial  $^{143}\text{Nd}/^{144}\text{Nd}$  ratios ( $\epsilon_{\text{Nd}}$  1.2 to 2.1) corresponding to group I kimberlites of South Africa. Their radiogenic Sr isotope ratios ( $^{87}\text{Sr}/^{86}\text{Sr}$  0.70537–0.70685) must be attributed to post-magmatic fluid overprint.

The syenitic sequence (nepheline syenite, foyaite, ijolite, hornblende syenite), a melilititic diatreme rock and the calciocarbonatite samples plot exclusively in the depleted mantle sector and form an array to progressively higher  $^{87}\text{Sr}/^{86}\text{Sr}$  ratios and lower  $\epsilon_{\text{Nd}}$  values (Fig. 10). Their Nd isotope range is remarkably narrow, given the wide petrographic rock spectrum and suggests a close genetic relationship. Like in other alkaline rock provinces (Harmer and Gittins 1998; Bizimis et al. 2003) the carbonatites have the most depleted isotopic compositions. The isotopic trend for the silicate rocks is not correlated to degree of magmatic fractionation. Major crustal contamination of the Sr and Nd isotope systems is unlikely for most of the Ayopaya samples because of their elevated strontium (e.g. >1,300 ppm Sr at the Cerro Sapo complex) and neodymium concentrations (>40 ppm Nd). The linear array stretches in between the two major mantle reservoirs HIMU and EM I (as defined by Zindler and Hart 1986) (Fig. 10). Similar linear trends can also be observed for most alkaline rocks in the East African rifts, e.g. Oldoinyo Lengai (Bell and Simonetti 1996) (Fig. 10). This trend either reflects mixing of two mantle components in a heterogeneous mantle plume (Bell and Tilton 2001), or mixing between a metasomatised EM-I type lithosphere and a plume-derived asthenospheric HIMU component (Bell and Simonetti 1996; Bizimis et al. 2003).

The composition of the most depleted magnesiocarbonatite sample from Ayopaya ( $\epsilon_{\text{Nd}}$  5.4,  $^{87}\text{Sr}/^{86}\text{Sr} = 0.70347$ ) is close to the HIMU reservoir (Fig. 10). Most magnesiocarbonatite samples plot in the range of plume-related oceanic island basalts such as Trindade Island (Siebel et al. 2000) (Fig. 1). These observations indicate that the Chiaracke magnesiocarbonatite represents an asthenospheric mantle component. The silicate rocks, but also the calciocarbonatites of the Ayopaya province

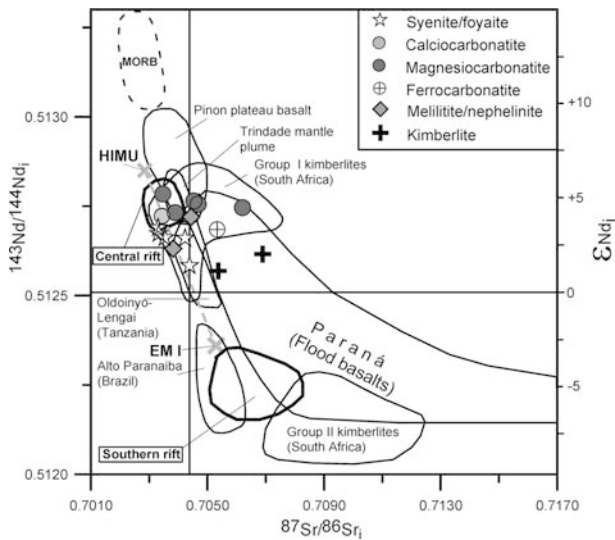


**Fig. 10** Sr–Nd-isotope diagram for rocks from the Ayopaya alkaline province (recalculated to  $t = 100$  Ma). Comparison with igneous rocks of similar age from South America and related rock types worldwide. Group I and II kimberlites (Kramers et al. 1981; Smith 1983), Oldoinyo Lengai (Bell and Dawson 1995), kamafugites and lamproites from Alto Paranaíba, SE Brazil (Gibson et al. 1995), Paraná flood basalts (Hawkesworth et al. 1986; Petrini et al. 1987), MORB (White and Hofmann 1982; O’Nions et al. 1977), HIMU and EM I (Hart et al. 1992), Central rift and Southern rift in Argentina (Lucassen et al. 2002). CHUR and Bulk Earth are recalculated from present-day values of 0.512638 and 0.7045, respectively, to 100 Ma

( $\epsilon_{Nd} \leq 4.1$ ), seem to represent a slightly different mantle source with a stronger contribution of an enriched component which may be the lithospheric mantle (EM-I like).

Similar to the alkaline complexes of East Africa, the Ayopaya province is part of a continental rift system (Fig. 1b). Samples of nephelinite and basanite from the prolongation of the Bolivian rift to northern Argentina at 25°S (“Central Rift” in Fig. 10, according to Lucassen et al. 2002) show the same depleted isotope signature as the most primitive samples from Ayopaya. The isotopic pattern of the rift-related Mesozoic rock suite is different from the isotopic composition of the subcratonic Mesozoic alkaline rocks from the Brazilian Shield (Fig. 10). The Brazilian samples from the Alto Paranaíba igneous province result from interaction of a mantle plume (e.g. Trindade hot spot, Fig. 1b) with the Archaean to Proterozoic lithospheric mantle (e.g. Gibson et al. 1995), whereas the rift-related Central Andean alkaline rocks reflect the non-cratonic Central Andean lithosphere as also seen in their Late Proterozoic to Palaeozoic model ages (Lucassen et al. 2002).

Most East African alkaline complexes show isotopic similarities between carbonatites and associated primitive silicate rocks (e.g. melilitites or olivine nephelinites), whereas the evolved silicate rock types show distinctly enriched isotopic compositions. This isotopic difference suggests that the carbonatites and the associated evolved silicate magmas developed as discrete “primary” melts

from the mantle (Harmer and Gittins 1998). In contrast, the isotopic similarity of carbonatites and evolved intrusive silicate rocks (foyaite, nepheline syenite) in the Cerro Sapo complex may indicate a largely mutual mantle source and differentiation by late-stage crustal processes, e.g. liquid immiscibility.

### Stable isotope data

The carbon and oxygen isotopic compositions of carbonatite samples from the Ayopaya province are given in Table 6 and plotted in Fig. 11. The data are presented as  $\delta^{13}C$  vs. PDB and  $\delta^{18}O$  vs. SMOW. The  $\delta^{13}C$  range of the magnesiocarbonatite samples from the Chiaracke intrusion and the ferrocarnatite samples ( $-4.9$  to  $-6.2\text{‰}$ ) corresponds to the primary igneous carbonatite field (Hoefs 1987), and the mantle field (Nelson et al. 1988; Deines 1989) (Fig. 11). The enriched  $\delta^{18}O$  values of these samples could be attributed to alteration processes and secondary isotopic exchange (Deines 1989; Keller and Hoefs 1995), e.g. weathering, and is similar to those of Mesozoic carbonatites from Brazil (Santos and Clayton 1995).

The calciocarbonatite samples from Ayopaya show an unusual trend of depletion in  $\delta^{13}C_{PDB}$  ( $-7.7$  to  $-9.2\text{‰}$ ) with increasing  $\delta^{18}O_{SMOW}$  ( $7.2$ – $11.0\text{‰}$ ), which correlates with degree of REE enrichment, and may be related to late-stage magmatic processes such as carbonate fractionation. Similar trends of  $^{13}C$  depletion have been reported from carbonatitic tuffs and lavas,

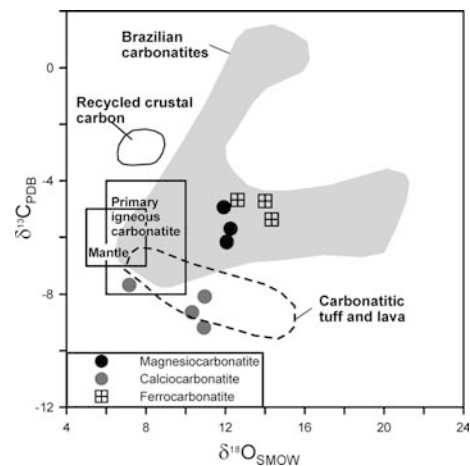


**Fig. 11** Stable isotope composition of carbonatite samples from the Ayopaya alkaline province. The magnesiocarbonatites and ferrocarnatites have similar ranges in oxygen and carbon isotope composition, while the calciocarbonatites from the Cerro Sapo complex are characterised by unusually low  $\delta^{13}C$ . Reference fields for Brazilian carbonatites are from Santos and Clayton (1995); carbonatitic tuff and lava is represented by Kaiserstuhl (Hay and O’Neil 1983) and Oldoinyo Lengai samples (Keller and Hoefs 1995). The compositional field for recycled crustal carbon is defined by carbonatites from Kerguelan Islands (Ray et al. 1999). Mantle and primary carbonatite fields are from Hoefs (1987), Nelson et al. (1988) and Deines (1989)

e.g. from Oldoinyo Lengai, Tanzania, and Kaiserstuhl, Germany (Fig. 11). The isotopic patterns of these rocks are attributed to secondary isotopic exchange by low-temperature alteration/recrystallisation, due to the instability of their natrocarbonates (Hay and O'Neil 1983; Keller and Hoefs 1995). Depletion in  $^{13}\text{C}$  can also result from isotopic fractionation between calcite and degassing  $\text{CO}_2$  (Suwa et al. 1975; Deines 1989), e.g. partitioning of heavy carbon into  $\text{CO}_2$  gas during hydrothermal exchange with  $\text{CO}_2$ -rich fluids (Chacko et al. 1991).

The calciocarbonatite and magnesiocarbonatite samples have distinctly different  $\delta^{13}\text{C}$  values which cannot entirely be attributed to secondary processes because of their similar postmagmatic history. Instead, these differences probably reflect different magmatic histories (see below).

### Carbonatite petrogenesis

The rock spectrum of the Ayopaya province can be regarded as a paradigm for carbonatite petrogenesis with examples of all three extensively debated models for carbonatite petrogenesis, i.e. primary carbonatitic mantle melts, carbonatites by liquid immiscibility from carbonated silicate melt, and carbonatite as product of crystal fractionation (residual liquid from advanced crystallisation).

#### *The Chiaracke magnesiocarbonatite as primary mantle melt*

The Chiaracke intrusion shows a number of features suggestive of an origin as a primary carbonatitic mantle melt from a depth of more than 70 km. These are:

*Field relationships* The 2-km<sup>2</sup>-large intrusive body shows no direct association with magmatic silicate rocks, contrary to the Cerro Sapo complex with its calciocarbonatite suite.

*Major element composition* High magnesium content, i.e. dolomitic composition, and very low  $\text{SiO}_2$  content (Fig. 4) correspond to experimentally defined primitive mantle melts (Wallace and Green 1988; and many others).

*REE distribution pattern* The Chiaracke samples have very steep REE distribution patterns when compared to other carbonatite samples from world-wide localities (Hornig-Kjarsgaard 1998) and to calciocarbonatite from the Cerro Sapo (Fig. 5). Their slope is similar to the kimberlite dyke which is very close to average kimberlite composition (Mitchell 1986) (Fig. 5b). The typical steep REE pattern of kimberlites is commonly attributed to the presence of residual garnet during low-degree partial melting of garnet lherzolite (e.g. Alibert et al. 1983; Ringwood et al. 1992). The magnesiocarbonatites have a REE distribution pattern parallel to the kimberlite but are enriched by a factor of about 10 (Figs. 5b and 9).

Dalton and Presnall (1998) suggested close genetic links between magnesiocarbonatites and kimberlites. A much flatter REE distribution pattern is shown by all other silicate and carbonate rocks from Ayopaya (Fig. 5).

*Trace-element distribution pattern* Residual garnet in the source of the magnesiocarbonatite is also indicated by the element patterns in Fig. 6. The magnesiocarbonatite shows characteristically low abundances in Ta, Nb, Sr, Zr, HREE and Y. Partition coefficients for garnet/carbonatite melt (Sweeney et al. 1992) indicate that Ti, Zr, Y and the HREEs are strongly partitioned into garnet. The relatively strong depletion in Nb, Ta and HREEs (Fig. 6) represents a very remarkable feature of the magnesiocarbonatites from Chiaracke, also when compared with the average magnesiocarbonatite of Woolley and Kempe (1989). The strong negative titanium anomaly in Fig. 6 results from the low solubility of Ti in carbonatite melts (Sweeney et al. 1992), and the compatible behaviour of titanium with garnet and amphibole. The Chiaracke magnesiocarbonatite also meets the criteria for a primary carbonatitic mantle melt as defined by Rudnick et al. (1993), i.e. high La/Yb (> 500), very low Ti/Eu (< 5) and high Ca/Al (60–790).

*Neodymium isotope composition* The magnesiocarbonatite samples show the highest initial  $\epsilon_{\text{Nd}}$  values (4.8–5.4) of all rocks from the Ayopaya region. These values are high even when compared with the Cretaceous carbonatites of the East African rift systems which are suggested to have a plume source (Bell and Tilton 2001).

#### *The calciocarbonatites of the Cerro Sapo complex as a result of liquid immiscibility*

The calciocarbonatites of the Cerro Sapo complex can be attributed to liquid immiscibility of a carbonate-saturated parental silicate melt (melilititic to nephelinitic) under crustal pressure (according to the model of Le Bas 1989; Kjarsgaard and Hamilton 1989) and successive crystal fractionation of the carbonatite melt after segregation. Liquid immiscibility as a reasonable model for the generation of the Cerro Sapo alkaline complex is indicated by:

1. There is a close spatial relationship of calciocarbonatite with nepheline-syenitic rocks in the Cerro Sapo complex. A similar situation can also be observed for the other nepheline-syenitic complexes (Cerro San Cristóbal, Cerro Quenamari) of the Ayopaya alkaline province (Fig. 1). At a metre-scale, some melilititic diatremes host small carbonatite lenses.
2. The calciocarbonatites of the Cerro Sapo intrusion are alkali-poor and their high calcic-carbonate content (> 85 wt%  $\text{CaCO}_3$ ) excludes a primary mantle origin, but indicates late-stage crustal processes, i.e. liquid immiscibility under crustal pressures (Lee and Wyllie 1997).

3. The trace-element distribution is consistent with liquid immiscibility plus subsequent crystal fractionation. Figure 6 shows two stages of calciocarbonatite evolution on the background of nepheline syenite composition. The first stage, as exemplified by sample I62, results in more or less equal amounts of Th, U, Ta, Nb, Zr, Y and middle and heavy rare-earth elements in the silicate and carbonate fraction. On the other hand, there is a pronounced enrichment of strontium, phosphorus and LREEs in the carbonate phase. This situation is in accordance with the experimental results by Hamilton et al. (1989), Jones et al. (1995) and Veksler et al. (1998b) who determined partitioning coefficients for co-existing silicate-carbonate liquids. Crystal fractionation then modifies the composition of the segregated carbonate liquid (second stage; sample I40) as portrayed by variable degree of REE, Th, Ba and Nb enrichment in accordance with the incompatible behaviour of these elements in a low-pressure carbonate melt-calcite system (Kjarsgaard and Hamilton 1989). The REE patterns of the calciocarbonatite samples are similar to those of the intrusive silicate rocks of the Cerro Sapo complex (average syenite/foyaite in Fig. 5b). The difference is in the degree of total REE enrichment and a slightly stronger LREE/HREE fractionation of the carbonatites.
4. A close genetic relationship between calciocarbonatites and syenites/foyaite of the Cerro Sapo complex is also indicated by their similar Nd-Sr isotopic composition (see above).

*The sodalite-ankerite-baryte dyke of the Cerro Sapo-complex as the result of extreme crystal fractionation of a carbonated silicate melt*

The sodalite-ankerite-baryte dyke of the Cerro Sapo complex represents an exotic and so far unique hybrid carbonate-silicate rock (Table 3) with very variable contents of the three main mineral components. The narrow rhythmic sodalite-ankerite layering and fluidal textures (Fig. 3) of the dyke suggest crystallisation from a silicate-rich carbonatitic melt system.

A genetic relationship between the sodalite-ankerite-baryte dyke and the intrusive silicate stock of the Cerro Sapo complex appears likely in view of the ubiquitous occurrence of sodalite in both rocks and their spatial association. Sodalite clearly represents the latest magmatic solidus phase of the nepheline-syenitic rocks. Inclusions of carbonate microcrysts in late-stage sodalite crystals of some foyaites indicate carbonate saturation of the late-stage residual magma. Additionally to the high carbonate content the occurrence of sodalite documents a strong enrichment in sodium and chlorine of the residual melt (sodalite has up to 24 wt% Na<sub>2</sub>O and 5 wt% Cl, Table 2). The parental magma was possibly pre-enriched in alkalis (especially Na) due to the prior separation of an immiscible calciocarbonatite liquid

(Kjarsgaard and Hamilton 1989). High magmatic barium contents like those of the sodalite-ankerite-baryte dyke (maximum 10–15 wt% BaO) have also been reported from other carbonatite occurrences, e.g. Mountain Pass, USA, and have been experimentally reproduced (Jones and Wyllie 1983; Mariano 1989).

Radiogenic as well as stable isotope data of the dyke indicate a mantle origin of the carbonate component of the dyke. The  $\epsilon_{\text{Nd}}$ -value of the ferrocarnatite-component of the dyke (I22 in Table 5,  $\epsilon_{\text{Nd}}$  3.4) is well in the range of the other samples from the Cerro Sapo complex ( $\epsilon_{\text{Nd}}$  2.9–3.5) indicating a common depleted mantle source. The mantle origin of the carbonate component of the dyke is also confirmed by a  $\delta^{13}\text{C}$ -value of  $-4.7\text{‰}$  (Table 6, Fig. 11).

The sodalite-ankerite-baryte dyke may be interpreted to represent the highly fractionated, fluid- and carbonate-rich, peralkaline residual melt or “flotation cumulate” (Ussing 1912; Markl et al. 2001) of the nepheline syenitic intrusion of the Cerro Sapo complex. However, the extreme enrichment in sodium and chlorine could also be understood as a result of exsolution and condensation of a H<sub>2</sub>O-CO<sub>2</sub>-rich fluid from a carbonated silicate melt, as recently suggested for the Oldoinyo Lengai natrocarbonatite lava flows by Nielsen and Veksler (2002).

*Cretaceous natrocarbonatite volcanism in the Ayopaya-province? Similarities to Oldoinyo Lengai, Tanzania*

The sodalite-ankerite-baryte dyke of the Cerro Sapo complex has many geochemical and petrological features in common with the natrocarbonatite lavas of Oldoinyo Lengai in Tanzania. The intrusive Cerro Sapo complex as well as the Oldoinyo Lengai volcano occur in a continental rift environment and are characterised by a similar alkaline assemblage comprising nephelinite, phonolite, nepheline syenite, ijolite, soevite (Dawson 1962; Dawson et al. 1995; Bell and Keller 1995).

The natrocarbonatites of Oldoinyo Lengai and the sodalite-ankerite-baryte dyke of the Cerro Sapo complex are unique in their unusual mineralogical and geochemical composition. Despite distinct differences in their mineral paragenesis they show an intriguing similarity in their characteristic element signatures. Both occurrences reflect late magmatic, fluid-rich systems which can be attributed to carbonate-rich alkaline silicate magmatism and which are characterised by unusual enrichment in Na, Cl, Ba, Sr, F, Br (for the sodalite-ankerite-baryte-dyke see Table 3, for Oldoinyo Lengai see Bell and Keller 1995). The carbonatite lavas predominantly consist of the two natrocarbonates gregoryite (Na<sub>2</sub>, K<sub>2</sub>, Ca, Sr, Ba)CO<sub>3</sub> and nyerereite (Na, K)<sub>2</sub>(Ca, Sr, Ba)(CO<sub>3</sub>)<sub>2</sub>, sylvine and fluorite (Dawson 1962; Keller and Krafft 1990; Dawson et al. 1995). The solidus of the natrocarbonate melt is reached at < 635 °C at 1–2 kbar (Petibon et al. 1998), or 650 °C at 1 kbar, respectively (Cooper et al. 1975). At pT-conditions higher than the natrocarbonate solidus a

silicate-bearing (natro)carbonatitic melt (> 5 wt% SiO<sub>2</sub> according to Petibon et al. 1998) will first precipitate alkali-rich silicate minerals such as nepheline, combeite, vishnevitte, coexisting with carbonate melt (e.g. Kjarsgaard et al. 1995; Petibon et al. 1998).

The textures of the sodalite-ankerite-baryte dyke (Fig. 3) indicate concomitant precipitation of carbonate and silicate phases, and the sodalite-ankerite-baryte dyke of the Cerro Sapo complex can possibly be interpreted as the intrusive equivalent of the recent natrocarbonatite lavas from Oldoinyo Lengai. The petrogenesis of these natrocarbonatites (liquid immiscibility vs. “expulsion of a cognate mobile, alkaline, CO<sub>2</sub>-rich fluid condensate”) is still much debated (e.g. Nielsen and Veksler 2002).

## Conclusions

The Ayopaya alkaline province is the petrologically most exotic expression of large-scale Mesozoic continental rifting along the western South American continent. This situation is similar to the still ongoing rifting in eastern Africa. However, the intracontinental rift evolution of South America represents failed rifts on an active convergent margin, whereas the East African rift magmatism is attributed to mantle plume activity. The Central Andean rift is probably related to plate reorganization in the Pacific region, i.e. a change in subduction from southeastward to northeastward with concomitant crustal attenuation at 80–120 Ma (Jaillard et al. 2000; Sempere et al. 2002).

Neodymium–strontium isotopes indicate mixing between an isotopically depleted asthenospheric mantle and a more enriched mantle component. The asthenospheric mantle is reflected by the magnesiocarbonatite intrusion of Chiaracke which is believed to derive from primary mantle melts (from depth > 70 km) that formed by low-degree partial melting of carbonated peridotite (garnet lherzolite). The survival of magnesiocarbonatite melt on ascent to shallow levels requires metasomatically prepared channelways of wehrlitic to clinopyroxenitic composition (Harmer and Gittins 1997; Wyllie and Lee 1998). Xenoliths of wehrlite and clinopyroxenite occur in ultramafic dykes and diatremes from Ayopaya, but also in other parts of the western South American rift zone. However, carbonatite and kimberlite magmatism is exclusively known from the Ayopaya area.

The least evolved silicate variants from partial melting of metasomatised and carbonate-rich mantle are represented by melilititic and nephelinitic rocks. These are alkali- and carbonate-rich, predominantly sodic, and show high contents in some trace elements (e.g. REE). Such parental melts further evolve into the broad spectrum of alkaline igneous rocks that characterises the Ayopaya province. The Cerro Sapo complex portrays the complexity of carbonatite magmatism, with calcio-carbonatite developing from carbonated nepheline sye-

nite melt by liquid immiscibility. The latest stage of nepheline syenite formation on extended crystal fractionation leads to a highly evolved fluid- and carbonate-rich residual melt which produces the sodalite-ankerite-baryte dyke system. The bewildering variety of rocks of different petrogenetic processes in the Ayopaya alkaline province reinforces the comment by Bell et al. (1998) “...there are carbonatites and carbonatites”.

**Acknowledgements** This study was funded by Deutsche Forschungsgemeinschaft (DFG), Gesellschaft für Technische Zusammenarbeit (GTZ) and Bundesanstalt für Geowissenschaften und Rohstoffe (BGR). We thank the National Survey for Mining and Geology (SERGEOMIN) of Bolivia for support during field work. Some Nd isotope analyses were done by Axel Höhndorf, Bundesanstalt für Geowissenschaften und Rohstoffe. Klaus Herrmann (Institute of Mineralogy and Mineral Resources, Technical University of Clausthal) helped with electron microprobe analysis. The manuscript benefited from critical reviews by Sally Gibson, Gerhard Brey, Thomas Stachel and Friedrich Lucassen.

## References

- Ahlfeld F (1966) Geologische Untersuchungen in der Provinz Ayopaya (Bolivien). *N Jb Mineral Abh* 104:147–171
- Ahlfeld F, Mosebach R (1935) Über Alkaligesteine in der bolivianischen Ostkordillere. *N Jb Mineral Geol Paläont* A69:388–414
- Ahlfeld F, Wegener R (1931) Über die Herkunft der im Bereich altperuanischer Kulturen gefundenen Schmuckstücke aus Sodalith. *Zeitschr Ethnologie* 63:288–296
- Alibert C, Michard A, Albrède F (1983) The transition from alkali-basalts to kimberlites: Isotope and trace element evidence from melilitites. *Contrib Mineral Petrol* 82:176–186
- Avila Salinas W (1989) Fases diastóricas y magmatismo Jurásico-Cretácico en Bolivia. *Bol Serv Geol Bolivia* A4(1): 47–68
- Bailey DK (1993) Carbonatite magmas. *J Geol Soc London* 150:637–651
- Balderrama Zárate BM (2003) Magmatismo mesozoico del complejo alcalino del Cerro Sapo. Tesis de grado Universidad Mayor de San Andrés, La Paz (in preparation)
- Bell K, Dawson JB (1995) Nd and Sr isotope systematics of the active carbonatite volcano, Oldoinyo Lengai. In: Bell K, Keller J (eds) Carbonatite volcanism: Oldoinyo Lengai and the petrogenesis of natrocarbonatites. IAVCEI Proceedings in volcanology, vol 4. Springer, Berlin Heidelberg New York, pp 100–112
- Bell K, Keller J (1995) Carbonatite volcanism. In: IAVCEI proceedings in volcanology, vol 4. Springer, Berlin Heidelberg New York, p 210
- Bell K, Simonetti A (1996) Carbonatite magmatism and plume activity: implications from the Nd, Pb, and Sr isotope systematics of Oldoinyo Lengai. *J Petrol* 37:1321–1339
- Bell K, Tilton GR (2001) Nd, Pb, Sr compositions of East African carbonatites: evidence for mantle mixing and plume inhomogeneity. *J Petrol* 42:1927–1945
- Bell K, Kjarsgaard BA, Simonetti A (1998) Carbonatites—into the twenty-first century. *J Petrol* 39:1839–1845
- Bergman SC (1987) Lamproites and other potassium-rich igneous rocks: a review of the occurrence, mineralogy and geochemistry. In: Fitton JG, Upton BG (eds) Alkaline igneous rocks. *Geol Soc London Spec Publ* 30:95–101
- Bizimis M, Salters VJM, Dawson JB (2003) The brevity of carbonatite sources in the mantle: evidence from Hf isotopes. *Contrib Mineral Petrol* 145:281–300
- Brendler W (1932) Über Sodalith vom Cerro Sapo, Bolivien. *Centralblatt Mineral Geol Paläont* A2:42–46

- Chacko T, Mayeda TK, Clayton RN, Goldsmith JR (1991) Oxygen and carbon isotope fractionation between CO<sub>2</sub> and calcite. *Geochim Cosmochim Acta* 55:2867–2882
- Clement CR (1982) A comparative geological study of some major kimberlite pipes in the Northern Cape and Orange Free State. PhD Thesis (2 vols), University of Cape Town
- Clement CR, Dawson JB, Geringer GJ, Gurney JJ, Hawthorne JB, Krol L, Kleinjan L, Zyl AA (1973) Guide for the first field excursion. International Conference on kimberlites, Cape Town
- Cooper AF, Reid DL (1998) Nepheline soevites as parental magmas in carbonatitic complexes: evidence from Dicker Willem, southwest Africa. *J Petrol* 39:2123–2137
- Cooper AF, Gittins J, Tuttle OF (1975) The system Na<sub>2</sub>CO<sub>3</sub>-K<sub>2</sub>CO<sub>3</sub>-CaCO<sub>3</sub> at 1 kilobar and its significance in carbonatite petrogenesis. *Am J Sc* 275:534–560
- Dalton JA, Presnall DC (1998) The continuum of primary carbonatitic kimberlitic melt compositions in equilibrium with lherzolite: data from the system CaO-MgO-Al<sub>2</sub>O<sub>3</sub>-SiO<sub>2</sub>-CO<sub>2</sub> at 6 GPa. *J Petrol* 39:1953–1964
- Dawson JB (1962) Sodium carbonate lavas from Oldoinyo Lengai, Tanganyika. *Nature* 195:865–879
- Dawson JB, Smith JV, Jones AP (1985) A comparative study of bulk rock and mineral chemistry of olivine melilitites and associated rocks from East and South Africa. *N Jb Mineral Abh* 152:143–175
- Dawson JB, Pinkerton H, Norton GE, Pyle DM, Browning P, Jackson D, Fallick AE (1995) Petrology and geochemistry of Oldoinyo Lengai lavas extruded in november 1988: magma source, ascent and crystallization. IAVCEI Proceedings in volcanology, vol 4. Springer, Berlin Heidelberg New York, pp 47–69
- Deines P (1989) Stable isotope variations in carbonatites. In: Bell K (ed) Carbonatites-genesis and evolution. Unwin-Hyman, London, pp 301–359
- Evensen NM, Hamilton PJ, O'Nions RK (1978) Rare earth abundances in chondritic meteorites. *Geochim Cosmochim Acta* 42:1199–1212
- Gibson SA, Thompson RN, Leonardos OH, Dickin AP, Mitchell JG (1995) The late Cretaceous impact of the Trindade mantle plume: evidence from large-volume, mafic, potassic magmatism in SE-Brazil. *J Petrol* 36:189–229
- Gittins J, Harmer RE (1997) What is ferrocarnatite? A revised classification. *J Afr Earth Sci* 1:159–168
- Hamilton DL, Bedson P, Esson J (1989) The behaviour of trace elements in the evolution of carbonatites. In: Bell K (ed) Carbonatite, genesis and evolution. Unwin Hyman, London, pp 405–427
- Hammerschmidt K, Döbel R, Friedrichsen H (1992) Implication of <sup>40</sup>Ar/<sup>39</sup>Ar-dating of early Tertiary volcanic rocks from the north-Chilean Precordillera. *Tectonophysics* 202:55–81
- Harmer RE, Gittins J (1997) The origin of dolomitic carbonatites: field and experimental constraints. *J Afr Earth Sci* 1:5–28
- Harmer RE, Gittins J (1998) The case of primary, mantle-derived carbonatite magma. *J Petrol* 39:1895–1903
- Hart SR, Hauri EH, Oschmann LA, Whitehead JA (1992) Mantle plumes and entrainment: isotopic evidence. *Science* 256:517–520
- Hawkesworth CJ, Mantovani MSM, Taylor PN, Palacz Z (1986) Evidence from the Parana of south Brazil for a continental contribution to Dupal basalts. *Nature* 322:356–359
- Hay RL, O'Neil JR (1983) Carbonatite tuffs in the Laetolil beds of Tanzania and the Kaiserstuhl in Germany. *Contrib Mineral Petrol* 82:403–406
- Hoefs J (1987) Stable isotope geochemistry, 3rd edn. Springer, Berlin Heidelberg New York, p 241
- Hornig-Kjarsgaard I (1998) Rare earth elements in sövitic carbonatites and their mineral phases. *J Petrol* 11/12:2105–2121
- Jaillard E, Héral G, Monfret T, Diaz-Martinez E, Baby P, Lavenue A, Dumont JF (2000) Tectonic evolution of the Andes of Ecuador, Peru Bolivia and northwestern Chile. In: Cordani UG, Milani EJ, Thomaz-Filho AT, Campos DA (eds) Tectonic evolution of South America. 31st International Geological Congress, Rio de Janeiro, pp 481–559
- Jones AP, Wyllie PJ (1983) Low temperature glass quenched from a synthetic rare-earth carbonatite: implications for the origin of the Mountain Pass deposit, California. *Econ Geol* 78:1721–1723
- Jones HJ, Walker D, Pickett DA, Murrell MT, Beattie P (1995) Experimental investigations of the partitioning of Nb, Mo, Ba, Ce, Pb, Ra, Th, Pa, and U between immiscible carbonate and silicate liquids. *Geochim Cosmochim Acta* 59:1307–1320
- Keller J, Hoefs J (1995) Stable isotope characteristics of recent natrocarbonatites from Oldoinyo Lengai. In: Bell K, Keller J (eds) Carbonatite volcanism: Oldoinyo Lengai and the petrogenesis of natrocarbonatites. IAVCEI proceedings in volcanology, vol 4. Springer, Berlin Heidelberg New York, pp 113–123
- Keller J, Krafft M (1990) Composition of natrocarbonatite lavas, Oldoinyo Lengai 1988. *Bull Volcanol* 52:629–645
- Kennan L, Lamb S, Rundle C (1995) K-Ar dates from the Altiplano and Cordillera Oriental of Bolivia: implications for Cenozoic stratigraphy and tectonics. *J South Am Earth Sci* 8:163–186
- Kjarsgaard B, Hamilton DL (1989) The genesis of carbonatites by immiscibility. In: Bell K (ed) Carbonatite, genesis and evolution. Unwin Hyman, London, pp 388–404
- Kjarsgaard BA, Hamilton DL, Peterson TD (1995) Peralkaline nephelinite/carbonatite liquid immiscibility: comparison of phase compositions in experiments and natural lavas from Oldoinyo Lengai. In: Bell K, Keller J (eds) Carbonatite volcanism: Oldoinyo Lengai and the petrogenesis of natrocarbonatites. IAVCEI Proceedings in volcanology, vol 4. Springer, Berlin Heidelberg New York, pp 163–190
- Kley J, Müller J, Tawackoli S, Jacobshagen V, Manutsoglu E (1997) Pre-Andean and Andean-age deformation in the Eastern Cordillera of southern Bolivia. *J South Am Earth Sci* 10:1–19
- Kramers JD, Smith CB, Lock NP, Harmon RS, Boyd FR (1981) Can kimberlite be generated from an ordinary mantle? *Nature* 291:53–56
- Le Bas MJ (1989) Nephelinitic and basanitic rocks. *J Petrol* 30:1299–1312
- Le Bas MJ, Le Maitre RW, Streckeisen AL, Zanettin B (1986) A chemical classification of volcanic rocks based on the total alkali-silica diagram. *J Petrol* 27:745–750
- Lee WJ, Wyllie PJ (1997) Liquid immiscibility in the join NaAl-SiO<sub>4</sub>-NaAlSi<sub>3</sub>O<sub>8</sub>-CaCO<sub>3</sub> at 1.0 GPa: implications for crustal carbonatites. *J Petrol* 38:1113–1135
- Lehmann B, Schultz F (1999) Diamanten und Alkaligesteine in den bolivianischen Ostanden. *Zeitschr angew Geol* 45:49–51
- Lucassen F, Escayola M, Romer RL, Viramonte J, Koch K, Franz G (2002) Isotopic composition of Late Mesozoic basic and ultrabasic rocks from the Andes (23–32 °S)—implications for the Andean mantle. *Contrib Mineral Petrol* 143:336–349
- Mariano AN (1989) Nature and economic mineralisation in carbonatites and related rocks. In: Bell K (ed) Carbonatite, genesis and evolution. Unwin Hyman, London, pp 149–172
- Markl G, Marks M, Schwinn G, Sommer H (2001) Phase equilibrium constraints on intensive crystallization parameters of the Illimaussaq complex, South Greenland. *J Petrol* 42:2231–2258
- Matos SR (1990) Los cuerpos de brecha ultramáfica (kimberlita) y los diques de diabasa del area de la Laguna Khoallaqui, Cochabamba, Bolivia. *Rev Tech YPFB* 11:259–265
- Matos SR (2000) El hallazgo de la carbonatita Chiaracke en la region de Independencia, Cochabamba: paper presented at XIII. Congr Geol Bol, La Paz
- McDonough WF, Sun S (1995) The composition of the earth. *Chem Geol* 120: 223–253
- Mitchell RH (1986) Kimberlites, mineralogy, geochemistry, petrology. Plenum, New York
- Moore AE, Erlank AJ (1979) Unusual olivine zoning. Evidence for complex physico-chemical changes during the evolution of olivine melilitite and kimberlite magmas. *Contrib Mineral Petrol* 70:391–405
- Nelson DR, Chivas AR, Chappell BW, McCulloch MT (1988) Geochemical and isotopic systematics in carbonatites and implications for the evolution of ocean-island sources. *Geochim Cosmochim Acta* 52:1–17

- Nielsen TFD, Veksler IV (2002) Is natrocarbonatite a cognate fluid condensate? *Contrib Mineral Petrol* 142:425–435
- O'Nions RK, Hamilton PJ, Evensen NM (1977) Variations in  $^{143}\text{Nd}/^{144}\text{Nd}$  and  $^{87}\text{Sr}/^{86}\text{Sr}$  ratios in oceanic basalts. *Earth Planet Sci Lett* 34:13–22
- Petibon CM, Kjarsgaard BA, Jenner GA, Jackson SE (1998) Phase relationships of a silicate-bearing natrocarbonatite from Oldoinyo Lengai at 20 and 100 MPa. *J Petrol* 39:2137–2151
- Petrini R, Civetta L, Piccirillo EM, Bellieni G, Comin-Chiaramonti P, Marques LS, Melfi AJ (1987) Mantle heterogeneity and crustal contamination in the genesis of low-Ti continental flood basalts from the Paraná plateau (Brazil): Sr-Nd isotope and geochemical evidence. *J Petrol* 28:701–726
- Ramos VA, Aleman A (2000) Tectonic evolution of the Andes. In: Cordani UG, Milani EJ, Thomaz-Filho AT, Campos DA (eds) *Tectonic evolution of South America*, 31st International Geological Congress, Rio de Janeiro, pp 635–685
- Ray JS, Ramesh R, Pande K (1999) Carbon isotopes in Kerguelen plume-derived carbonatites: evidence for recycled inorganic carbon. *Earth Planet Sci Lett* 170:205–214
- Ringwood AE, Kesson SE, Hibberson W, Ware N (1992) Origin of kimberlites and related magmas. *Earth Planet Sci Lett* 113:521–538
- Rudnick RL, McDonough WF, Chappell BW (1993) Carbonatite metasomatism in the northern Tanzanian mantle: petrographic and geochemical characteristics. *Earth Planet Sci Lett* 116:463–475
- Santos RV, Clayton RN (1995) Variations of oxygen and carbon isotopes in carbonatites: a study of Brazilian alkaline complexes. *Geochim Cosmochim Acta* 59:1339–1352
- Scheuber E, Charrier R, Gonzalez G, Klotz K-J (2000) Crustal evolution of the Southern Central Andes (20°S–26°S) since the Jurassic. *Zeitschr angew Geol* SH1:323–329
- Sempere T, Carlier G, Carlotto V, Jacay J (1998) Rifting Pérmico Superior—Jurássico Medio en la Cordillera Oriental de Perú y Bolivia. *Memorias XIII Congreso Geológico de Bolivia, Potosí—Bolivia*, Tomo I:31–37
- Sempere T, Carlier G, Soler P, Fornari M, Carlotto V, Jacay J, Arispe O, Néraudeau D, Cárdenas J, Rosas S, Jiménez N (2002) Late Permian-Middle Jurassic lithospheric thinning in Peru and Bolivia, and its bearing on Andean-age tectonics. *Tectonophysics* 34:153–181
- Siebel W, Becchio R, Volker F, Hansen MAF, Viramonte J, Trumbull RB, Haase G, Zimmer M (2000) Trindade and Martín Vaz Islands, south Atlantic. Isotopic (Sr, Nd, Pb) and trace element constraints on plume related magmatism. *J South Am Earth Sci* 13:79–103
- Smith CB (1983) Pb, Sr and Nd isotopic evidence of southern African Cretaceous kimberlites. *Nature* 304:51–54
- Smith CB, Gurney JJ, Skinner EMW, Clement CR, Ebrahim N (1985) Geochemical character of southern African kimberlites: a new approach based on isotopic constraints. *Trans Geol Soc Afr* 88:267–280
- Steiger RH, Jäger E (1977) Subcommittee on geochronology: convention on the use of decay constants in geo- and cosmochronology. *Earth Planet Sci Lett* 36:359–362
- Suwa K, Oana S, Wada H, Osaki S (1975) Isotope geochemistry and petrology of African carbonatites. *Phys Chem Earth* 9:735–745
- Sweeney RJ, Green DH, Sie SH (1992) Trace and minor element partitioning between garnet and amphibole and carbonatitic melt. *Earth Planet Sci Lett* 113:1–14
- Tompkins LA, Gonzaga GM (1989) Diamonds in Brazil and a proposed model for the origin and distribution of diamonds in the Coromandel region, Minas Gerais, Brazil. *Econ Geol* 84:591–602
- Ussing NV (1912) Geology of the country around Julianehaab, Greenland. *Meddelelser om Groenland* 38:1–426
- Veksler IV, Nielsen TFD, Sokolov SV (1998a) Mineralogy of crystallized melt inclusions from Gardiner and Kovdor ultramafic alkaline complexes: implications for carbonatite genesis. *J Petrol* 39:2015–2032
- Veksler IV, Petibon C, Jenner GA, Dorfman AM, Dingwell DB (1998b) Trace element partitioning in immiscible silicate-carbonate liquid systems: an initial experimental study using a centrifuge autoclave. *J Petrol* 39:2095–2104
- Viramonte JG, Kay SM, Becchio R, Escayola M, Novitski I (1999) Cretaceous rift related magmatism in central-western South America. *J South Am Earth Sci* 12:109–121
- Wallace ME, Green DH (1988) An experimental determination of primary carbonatite magma composition. *Nature* 335:343–346
- White WM, Hofmann AW (1982) Sr and Nd isotope geochemistry of oceanic basalts and mantle evolution. *Nature* 296:821–825
- Woolley AR, Kempe DRC (1989) Carbonatites: nomenclature, average chemical composition and element distribution. In: Bell K (ed) *Carbonatite, genesis and evolution*. Unwin Hyman, London, pp 1–14
- Woolley AR, Bergman SC, Edgar AD, Le Bas MJ, Mitchell RH, Rock NMS, Scott-Smith BH (1996) Classification of lamprophyres, lamproites, kimberlites, and the kalsilitic, melilititic, and leucitic rocks. *Can Mineral* 34:173–186
- Wyllie PJ, Lee W-J (1998) Kimberlites, carbonatites, peridotites and silicate-carbonate liquid immiscibility explained in parts of the system  $\text{CaO}-(\text{Na}_2\text{O} + \text{K}_2\text{O})-(\text{MgO} + \text{FeO})-(\text{SiO}_2 + \text{Al}_2\text{O}_3)-\text{CO}_2$ . In: *Seventh international kimberlite conference, extended abstracts*. Cape Town, pp 923–932
- Zindler A, Hart SR (1986) Chemical dynamics. *Annu Rev Earth Planet Sci* 14:496–571